Determination of the Spatial Distribution of Ozone Precursor and Greenhouse Gas Concentrations and Emissions in the LA Basin

Jochen Stutz[1]
Ross Cheung[1], Olga Pikelnaya[1,2], Santo Fedele Colosimo[1], Clare Wong[3,4], Dejian Fu[3], Thomas Pongetti[3], Stanley P. Sander[1,3,4]

[1]Joint Institute for Regional Earth System Science and Engineering, UCLA
[2] now at South Coast Air Quality Management District
[3]NASA Jet Propulsion Laboratory, California Institute of Technology
[4]Division of Geological and Planetary Sciences, California Institute of Technology

Two Environmental Challenges for LA and CA

Ozone levels above the Federal Air Quality Standard remains a challenge in the SCAB.

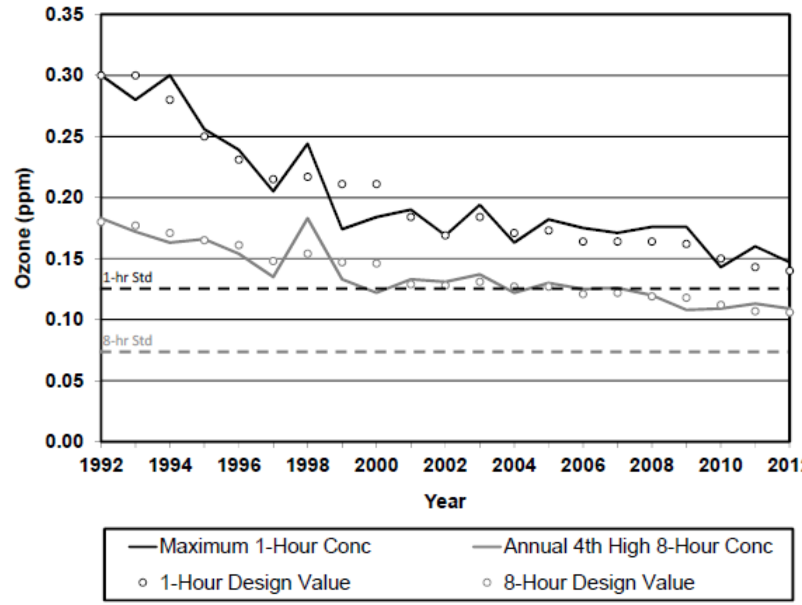

Climate change is driven by greenhouse gas emissions, many of which come from megacities like Los Angeles

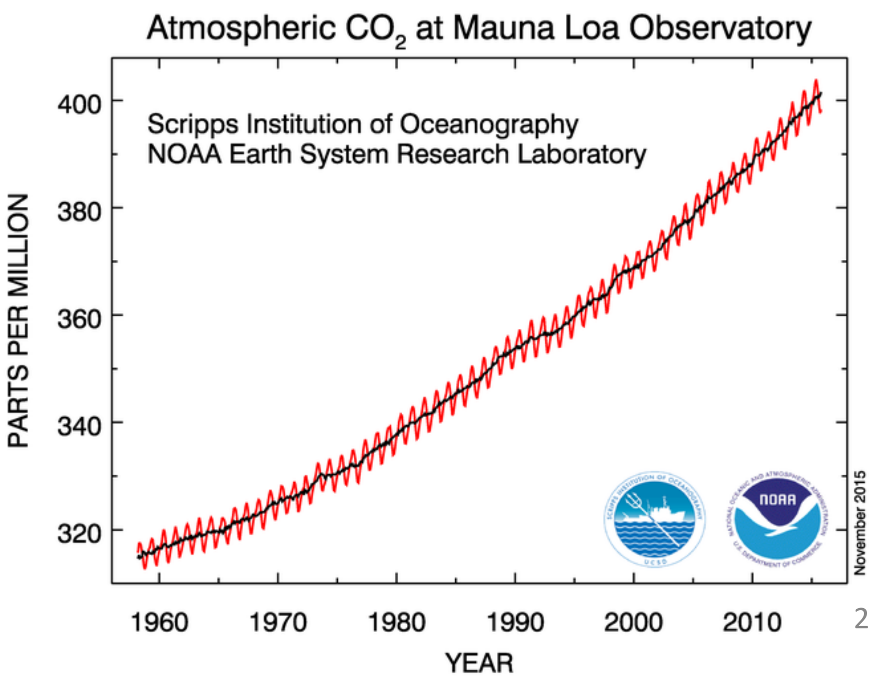

GHG and Ozone in Cities

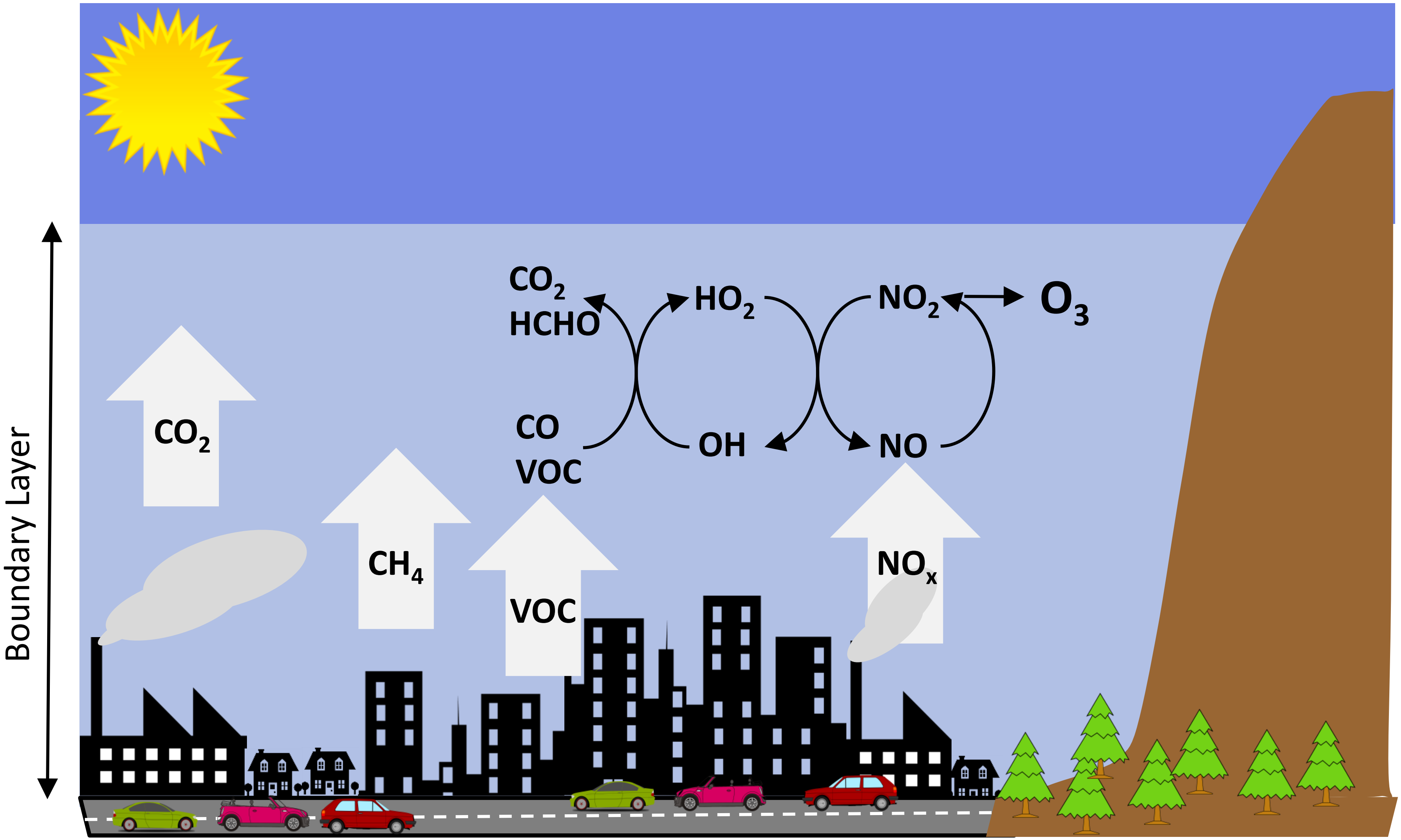

Monitoring of GHG, O_3, and O_3 precursors in Cities

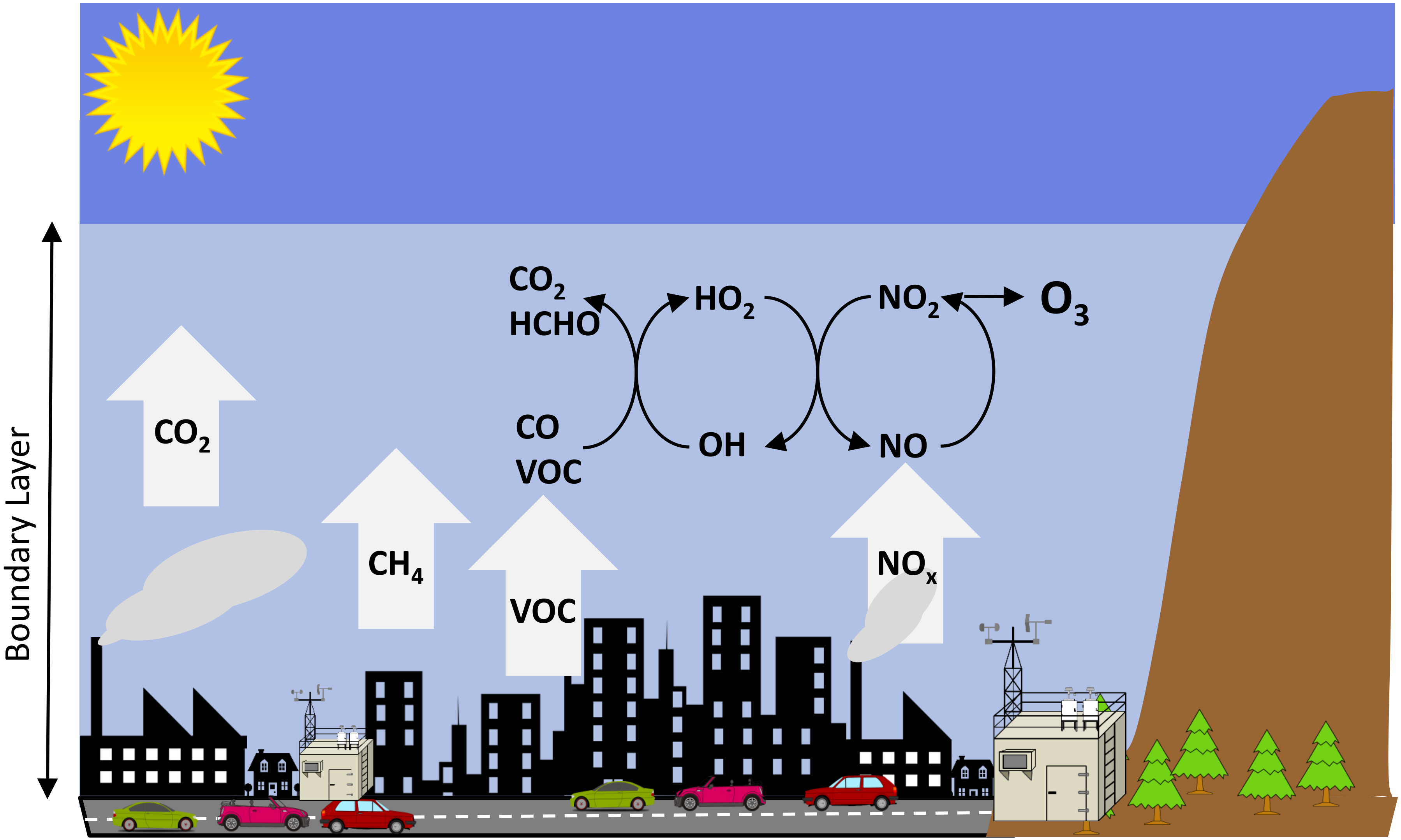

Motivation: Air Quality and GHG Monitoring

Ground stations have limited spatial coverage and are influenced by local emissions.

Satellite measurements have greater spatial coverage, but less sensitivity to measurements near surface, less temporal resolution.

No vertical information is available

GHG observational network is still very sparse

There is a need for long-term monitoring techniques of urban ozone precursors and greenhouse gases with good spatial and temporal resolution

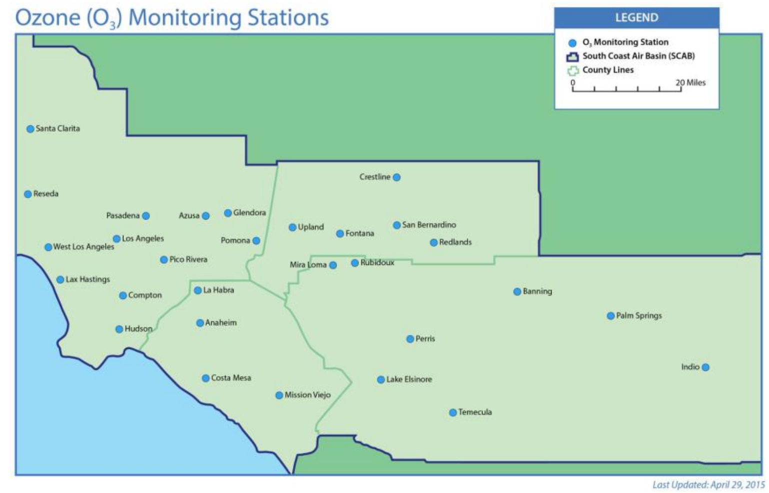

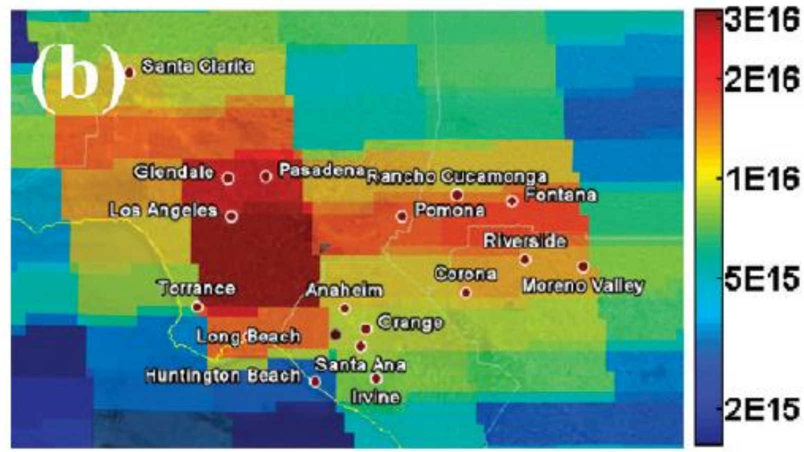

Tropospheric NO_2 columns from OMI Satellite over South Coast Region of California for one day, August 1, 2008.

From (Russell et al., 2010)

A New Approach

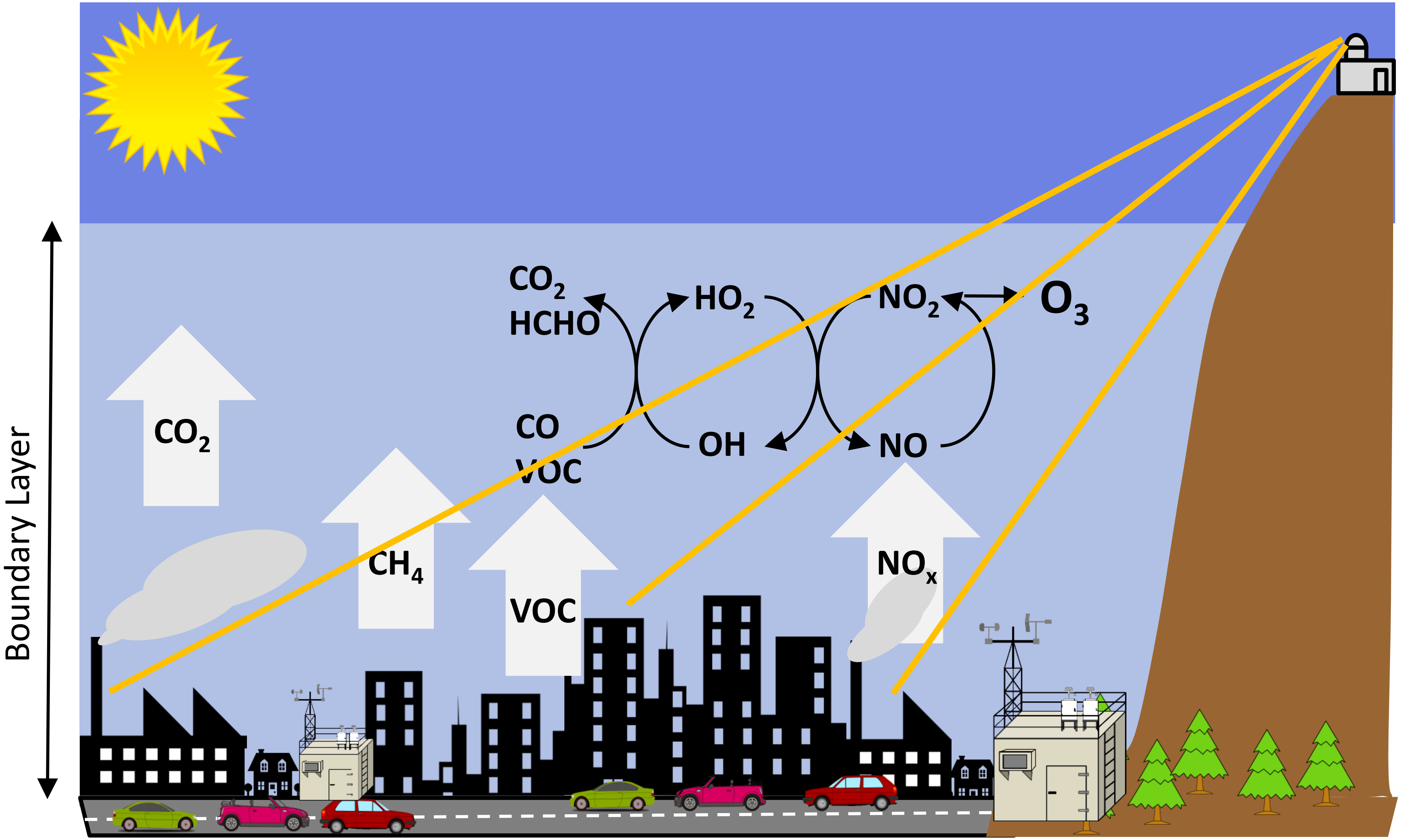

A New Approach

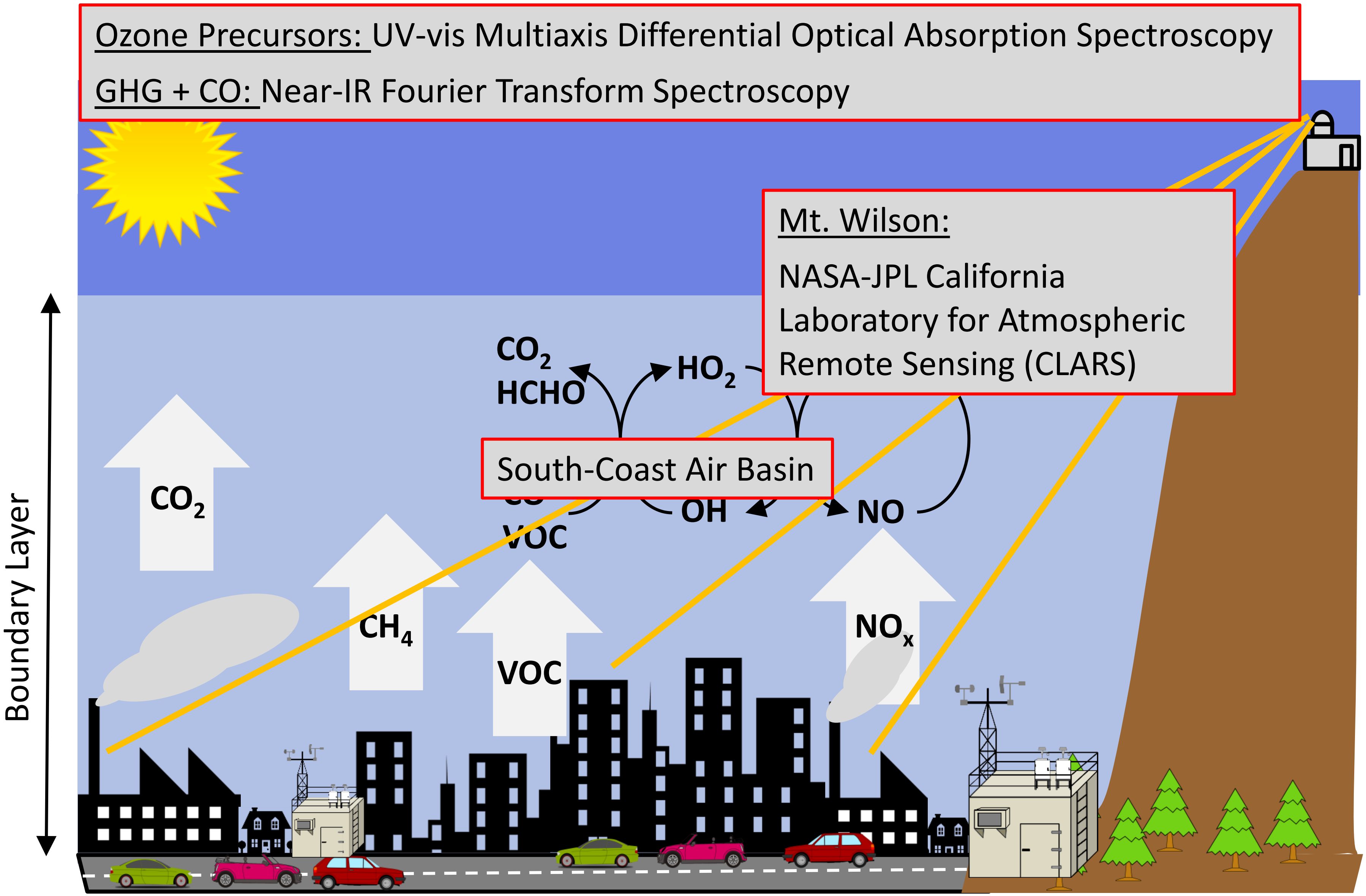

CLARS at Mt. Wilson

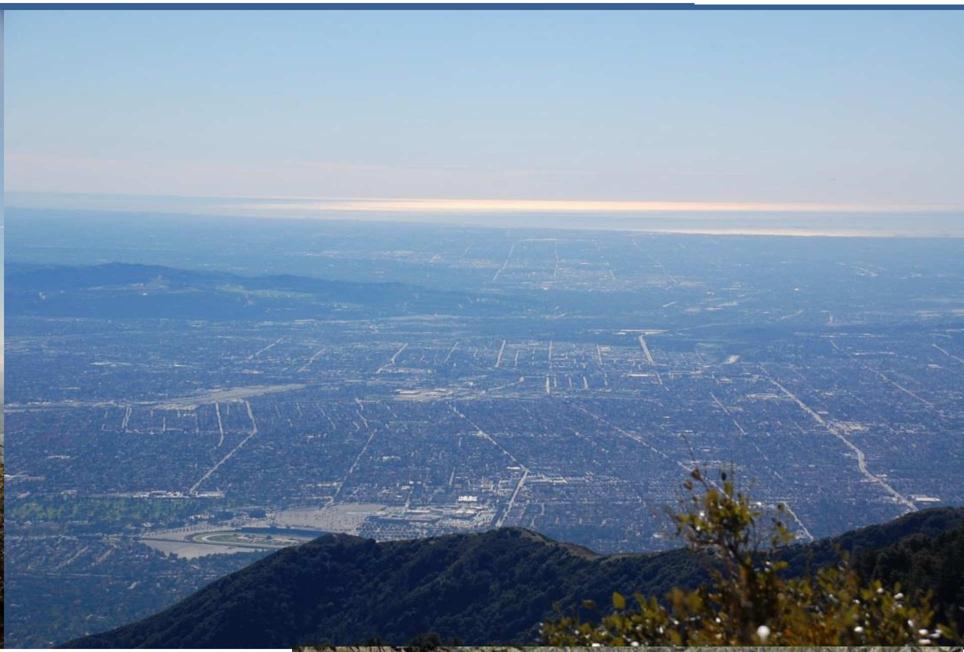

California Laboratory for Atmospheric Remote Sensing (CLARS)

Altitude: 1.7 km a.s.l.

Current Instrumentation:

- Multi-Axis DOAS
- Near-IR FTS
- In-situ GHG monitoring (ARB)
- Meteorology

Testbed for future geostationary satellites (Tempo).

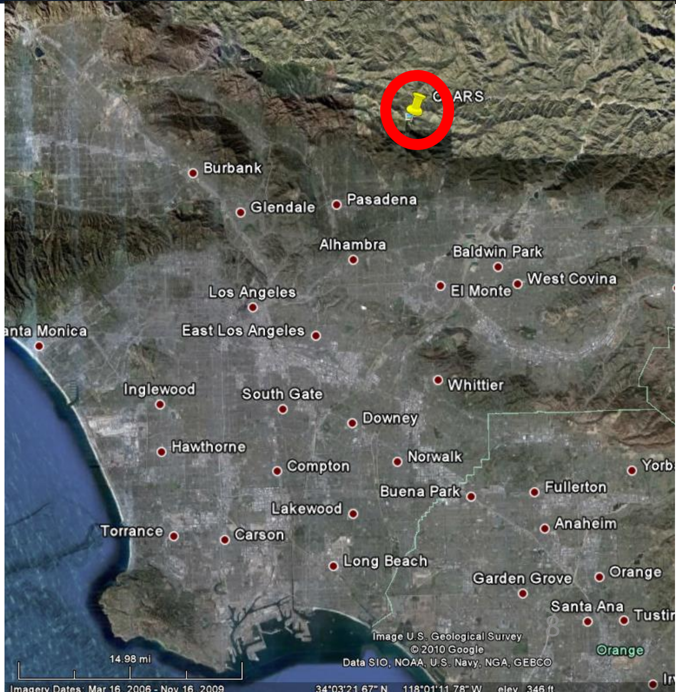

Multiaxis - DOAS

Continuous scans in both vertical (elevation) and horizontal (azimuth).
Cycle length: 60-80 minutes

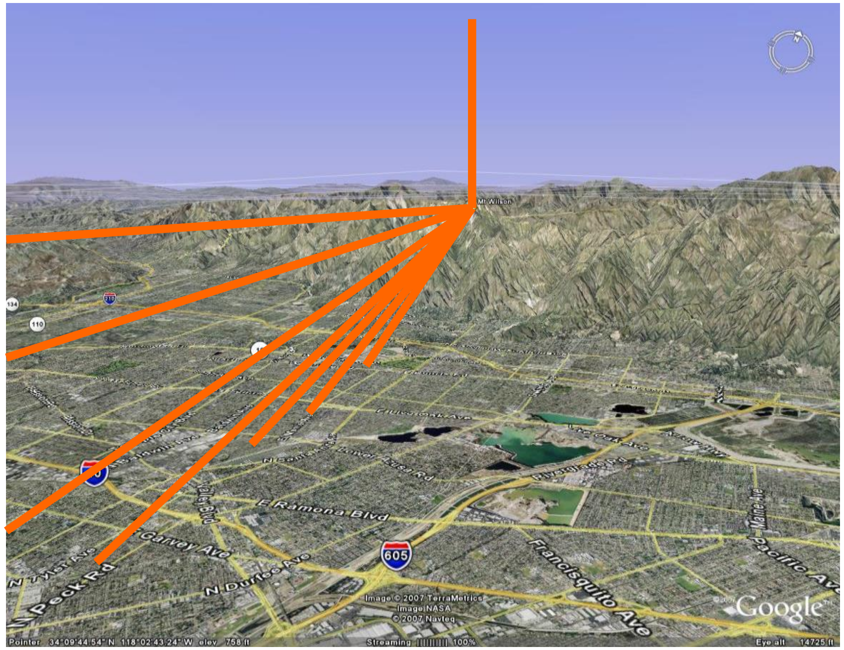

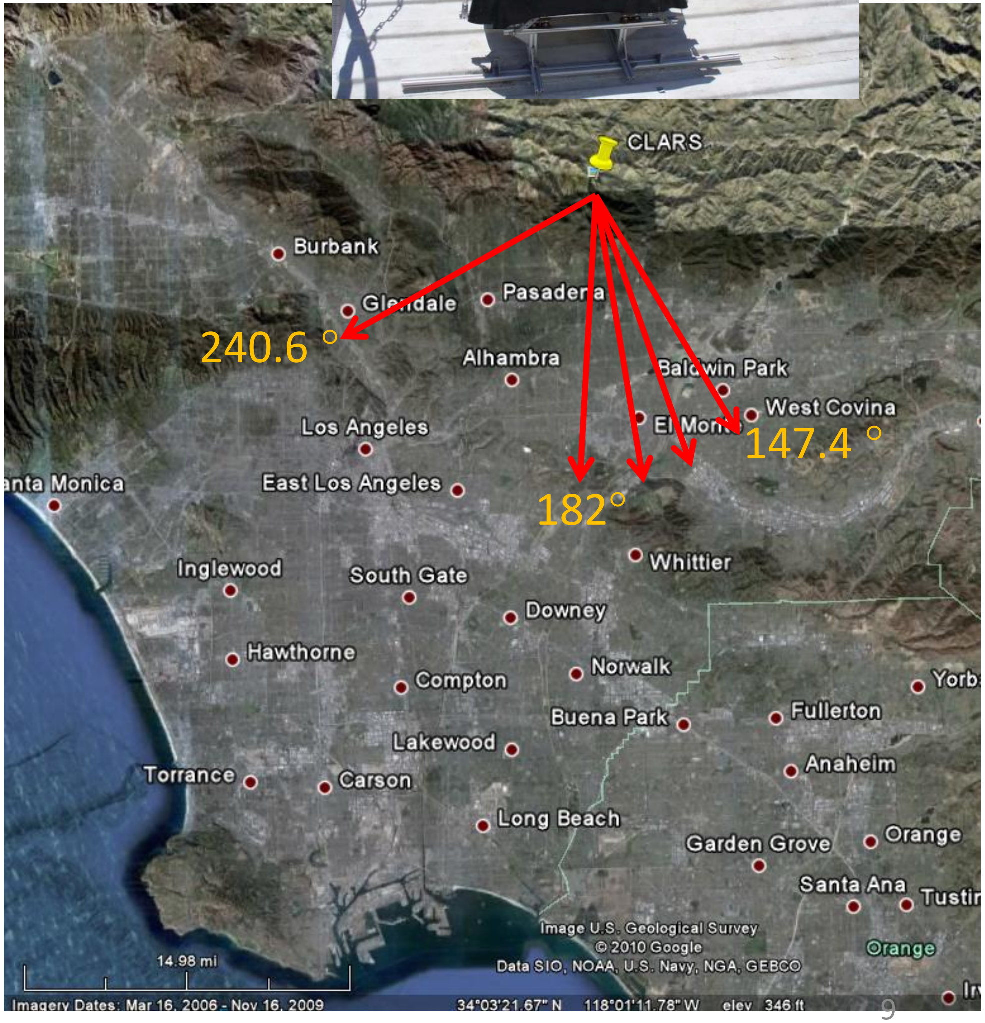

Azimuth Angles	147.4°, 160°, 172.5°, 182°, 240.6°
Elevation Angles	-10°, -8°, -6°, -4°, -2°, 0°, 3°, 6°, 90°

Differential Optical Absorption Spectroscopy

$$D' = \ln\left(-\frac{I(\lambda)}{I_0'(\lambda)}\right)$$

$$SCD = \frac{D'}{\sigma(\lambda)} = \int_{\text{absorption path}} \text{Conc.}(s)\, ds$$

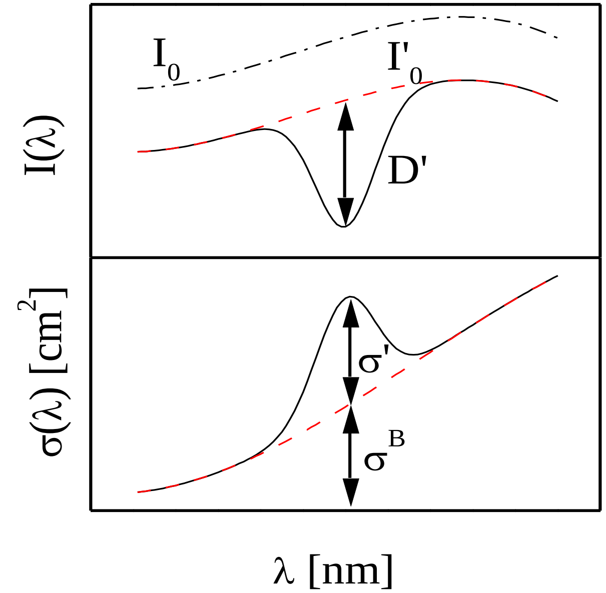

Multi-Axis DOAS (MAX-DOAS):
ground-based passive spectrometer, looking at a positive elevation angle α, collecting scattered sunlight

$$DSCD = SCD_{off-axis} - SCD_{zenith}$$

Differential slant column densities (DSCD) removes stratospheric absorptions and Solar Fraunhofer lines

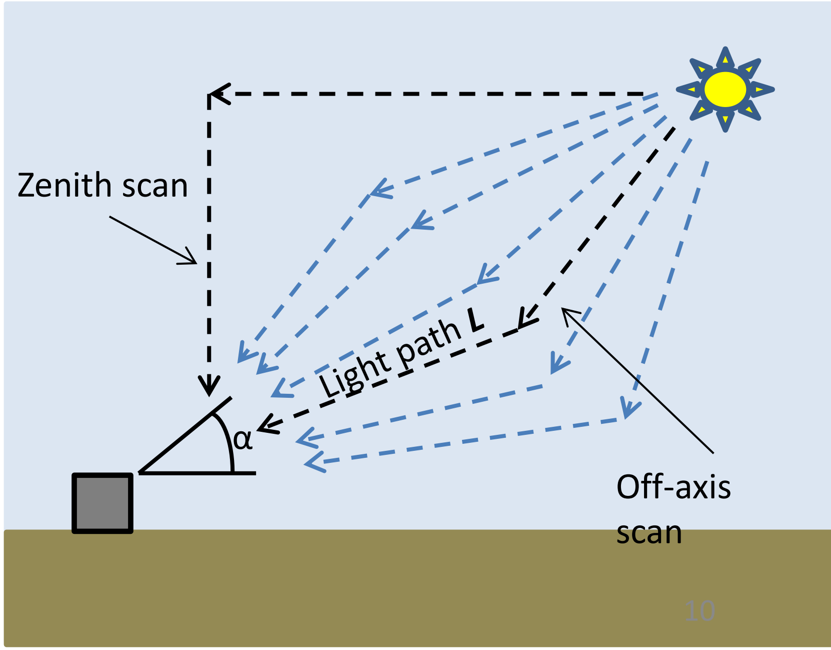

Trace Gases Measured

Species	Scan	Wavelength Interval (nm)	Fitted Spectral References	Detection Limit
O_4	UV	350-390	NO_2, O_4, HCHO, HONO	$7*10^{41}$ molec^2/cm^5
O_4	Vis	464-506.9	NO_2, glyoxal, O_4, H_2O	$8*10^{41}$ molec^2/cm^5
O_4	Vis	519.8 - 587.7	NO_2, O_4, O_3, H_2O	$5*10^{41}$ molec^2/cm^5
HCHO	UV	332.8-377.8	HCHO, NO_2,O_4, O_3, HONO	$2*10^{16}$ molec/cm^2
NO_2	UV	332.8-377.8	NO_2, HCHO, O_4, O_3, HONO	$2*10^{15}$ molec/cm^2
NO_2	UV	416.3-456.6	NO_2, glyoxal, O_4, H_2O	$1*10^{15}$ molec/cm^2
NO_2	Vis	464-506.9	NO_2, glyoxal, O_4, H_2O	$1*10^{15}$ molec/cm^2
NO_2	Vis	519.8 - 587.7	NO_2, O_4, O_3, H_2O	$2*10^{15}$ molec/cm^2

At each viewing angle the MAX-DOAS scans twice in two different wavelength ranges, once in the UV (335-465 nm), and once in the visible (465-595 nm)

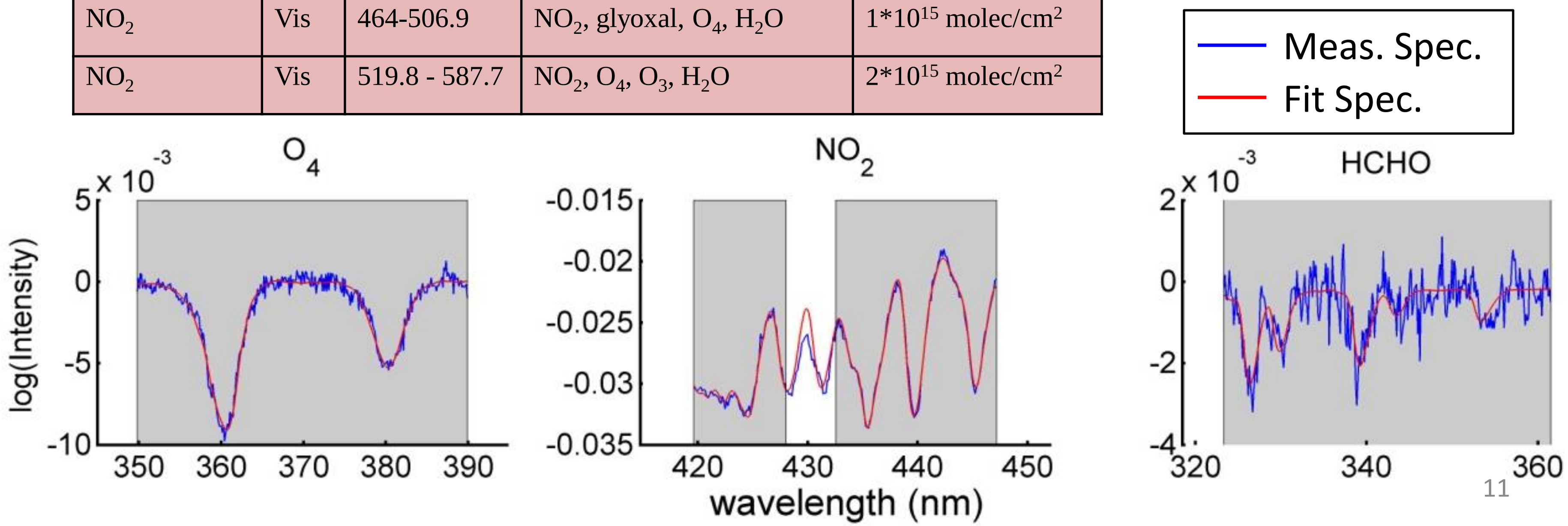

From Columm Densities to Concentrations

What does the MAX-DOAS “see”?

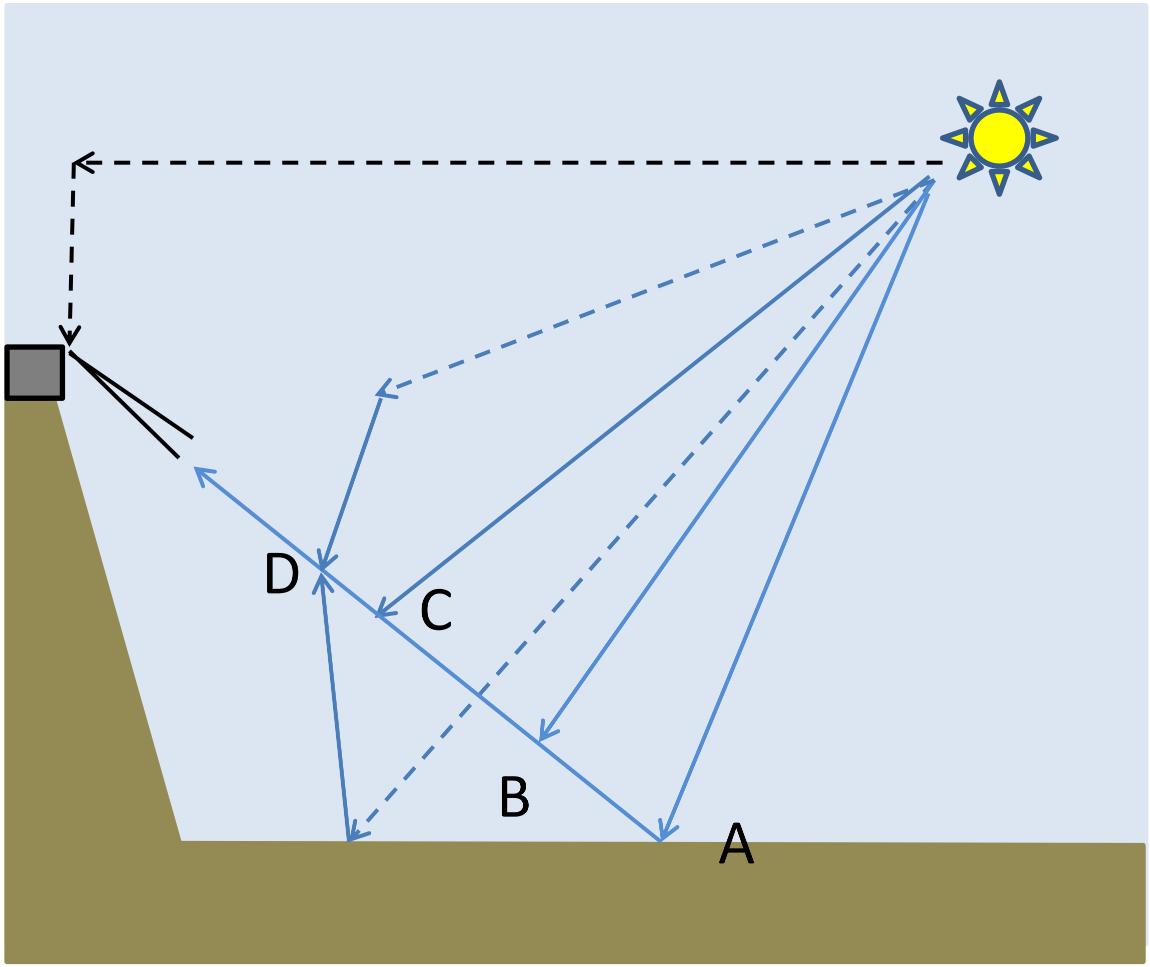

A: Reflection from the ground.

B: Rayleigh scattering by air molecules.

C: Mie scattering by aerosol

D: Multiple scattering events

- A model simulating the radiative transfer is needed in the UV and visible
- Use of a tracer for the radiative transfer can be used in the near-IR

Cloud Sorting

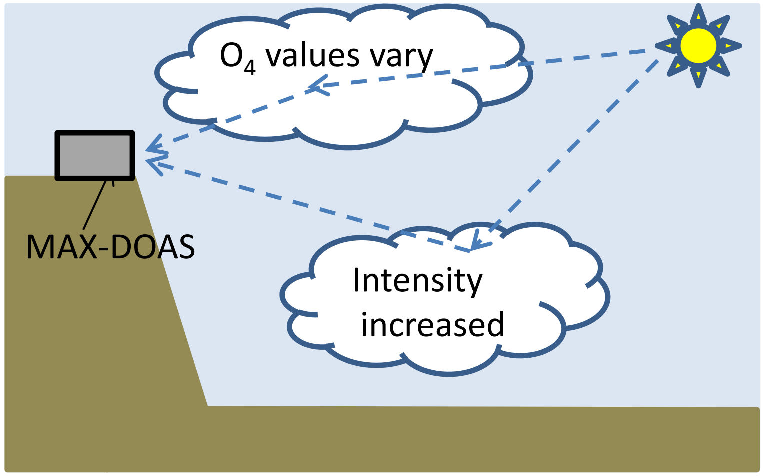

Low clouds: highly reflective, block view of basin

High clouds: Attenuation/ scattering light

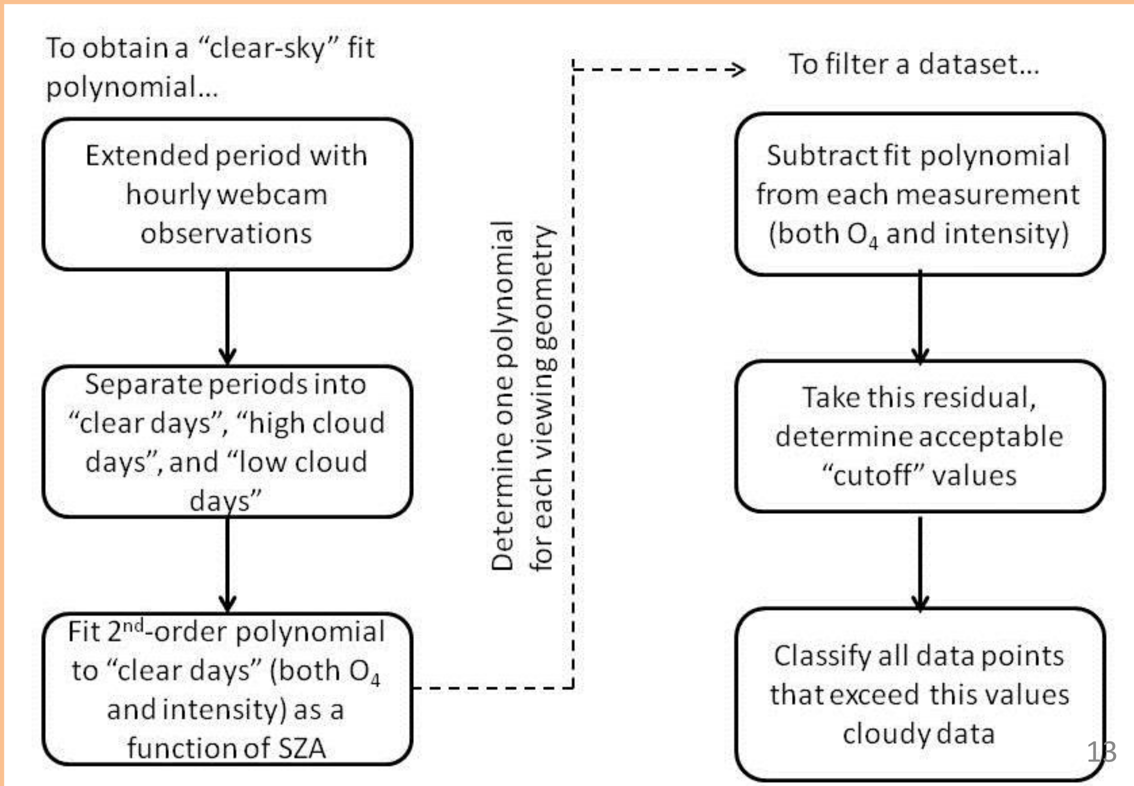

Qualitative Radiative Transfer Considerations

VLIDORT calculates **Differential Box Air-Mass Factors (DBAMF)** showing each atmospheric layer's contribution to absorption and scattering at each elevation angle:

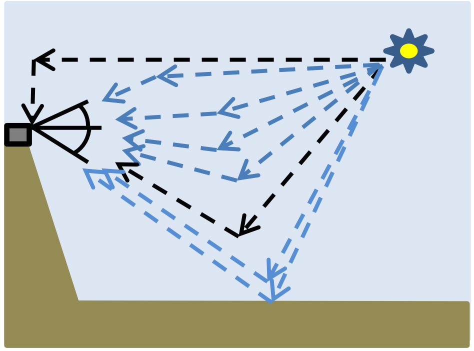

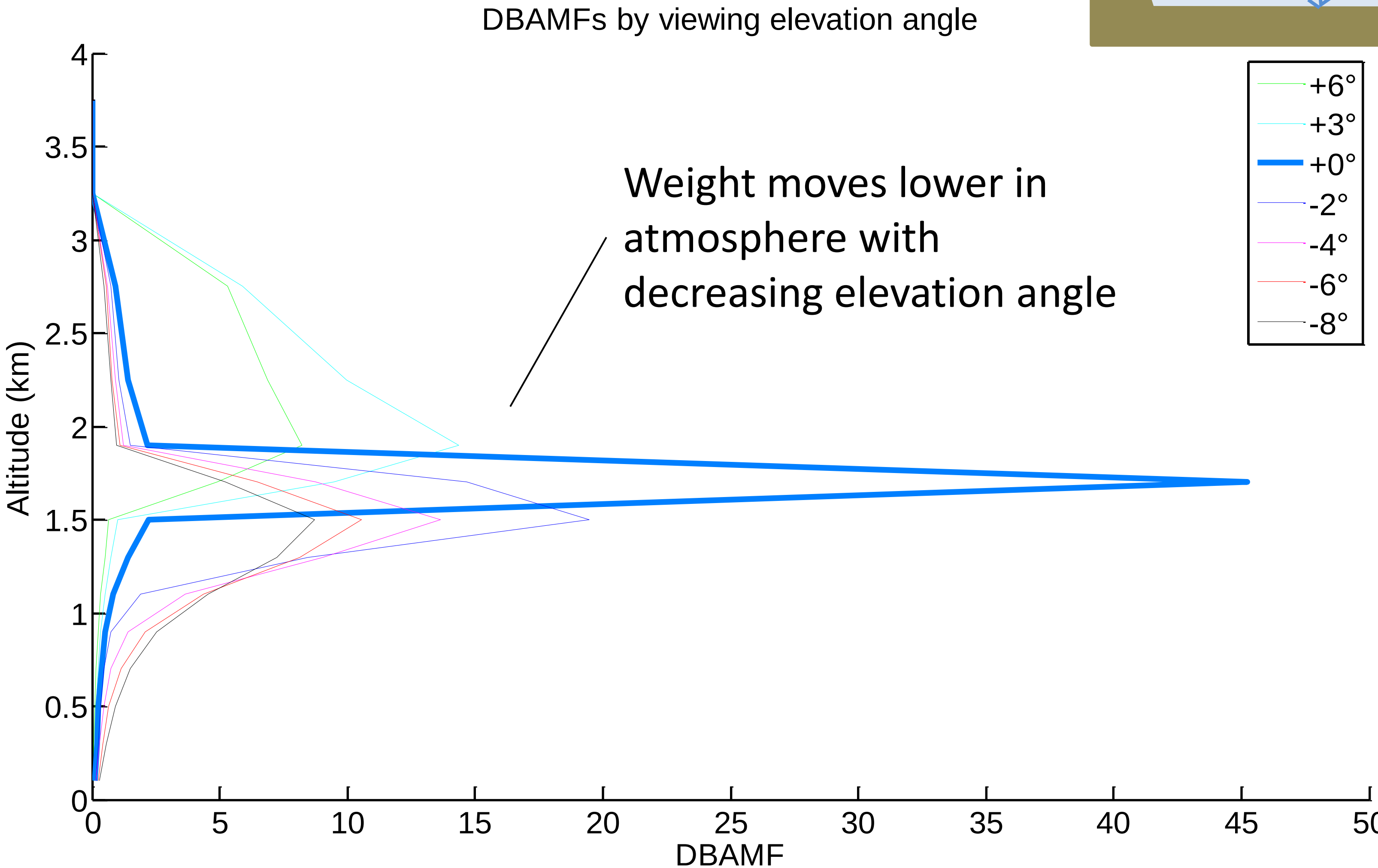

Qualitative Radiative Transfer Considerations

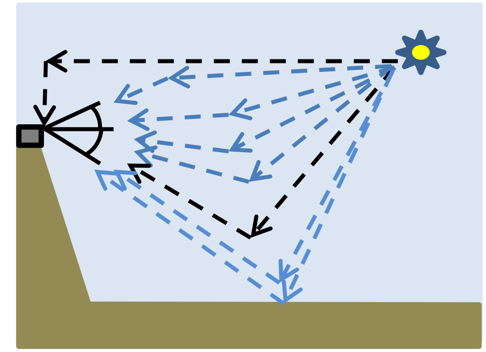

VLIDORT calculates **Differential Box Air-Mass Factors (DBAMF)** showing each atmospheric layer's contribution to absorption and scattering at each elevation angle:

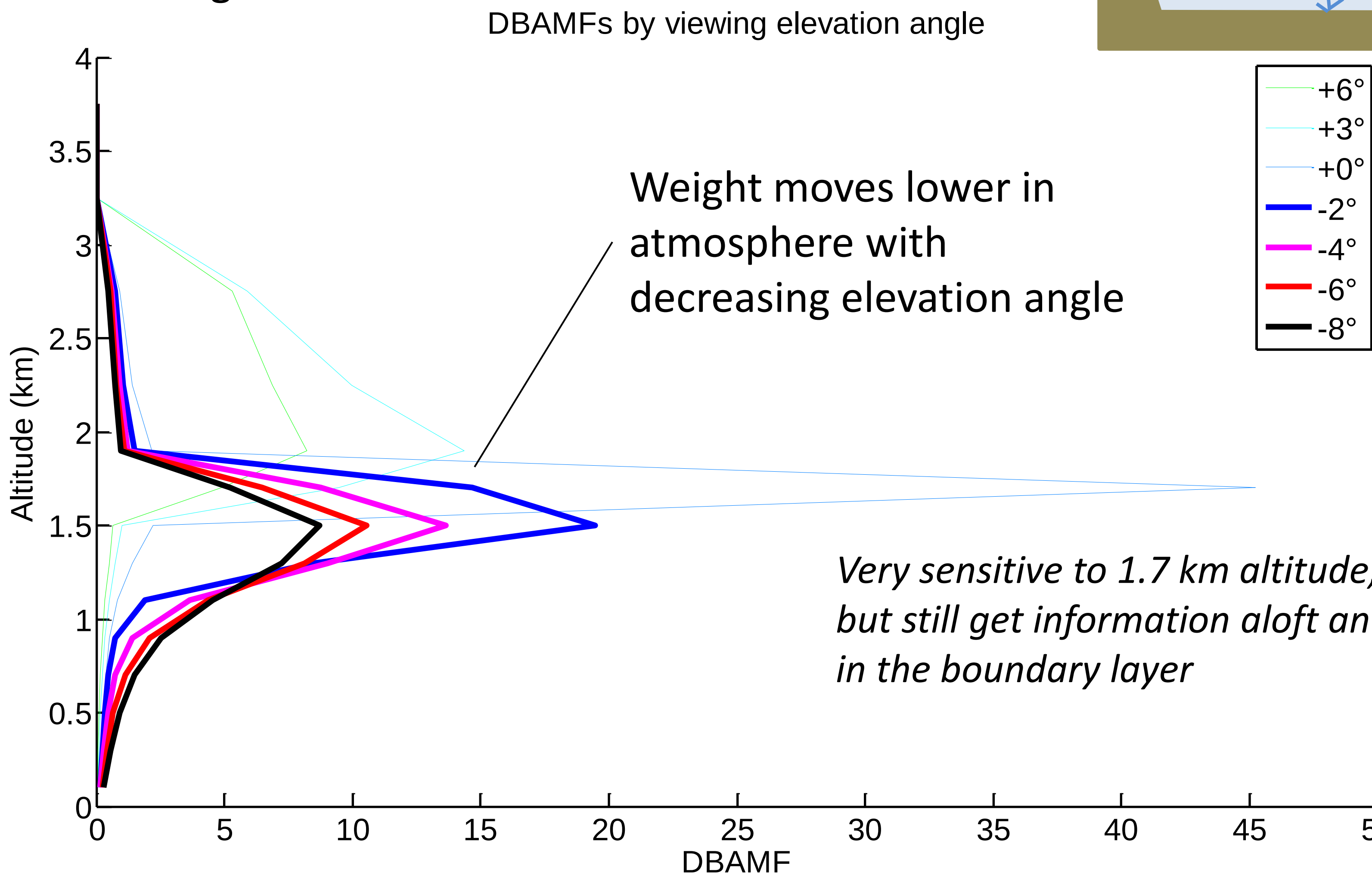

Weight moves lower in atmosphere with decreasing elevation angle

Very sensitive to 1.7 km altitude, but still get information aloft and in the boundary layer

Qualitative Radiative Transfer Considerations

VLIDORT calculates **Differential Box Air-Mass Factors (DBAMF)** showing each atmospheric layer's contribution to absorption and scattering at each elevation angle:

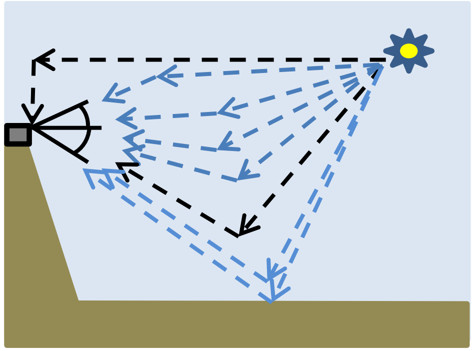

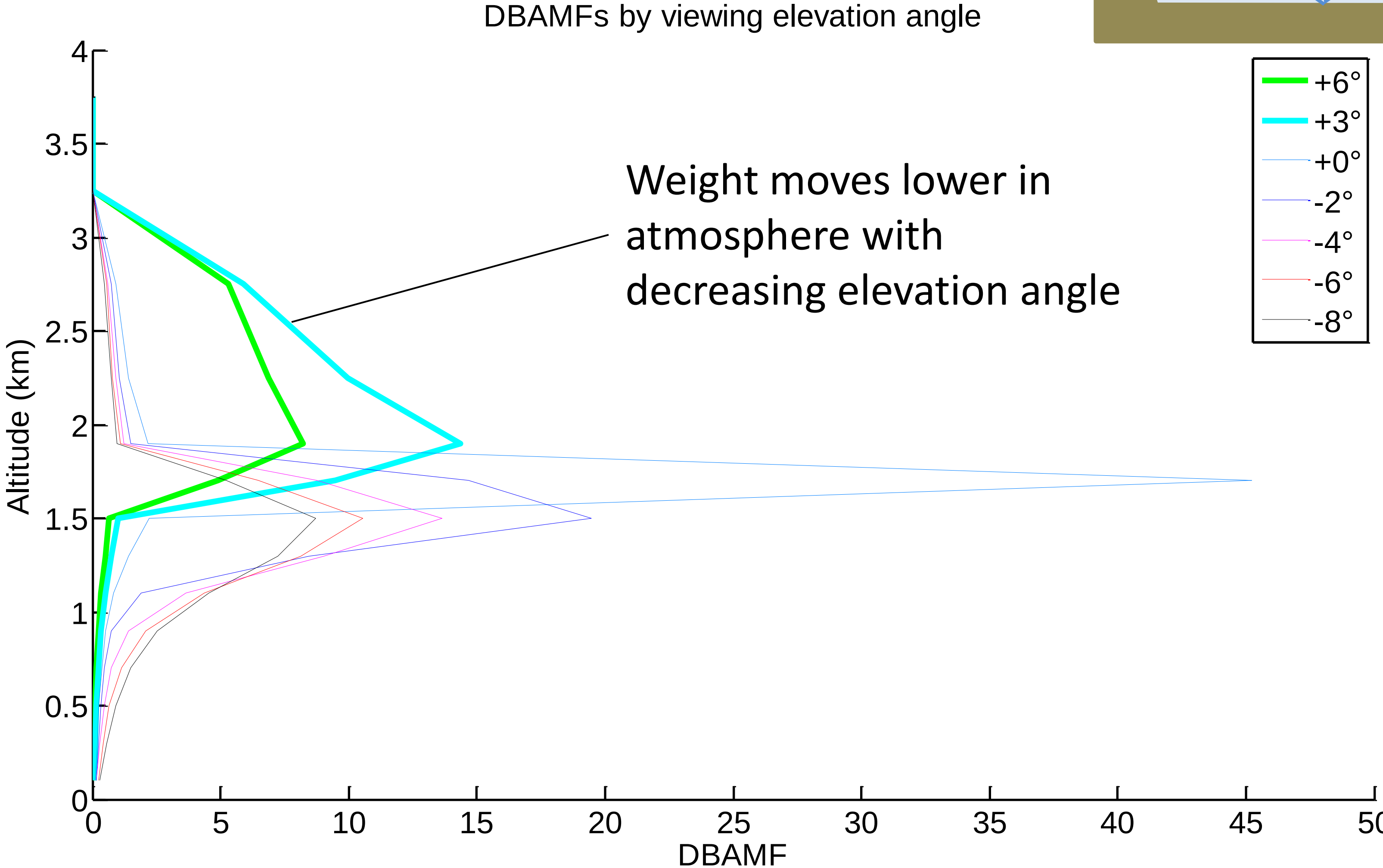

Quantitative Retrieval Approach

<u>Radiative Transfer Constraints:</u>

- O_4 DSCD+ non-linear optimal estimation
- Aerosol extinction profile from AERONET and LIDAR observations

<u>MAX-DOAS Observations:</u>

Trace gas slant column density at different viewing elevations

Radiative Transfer Model + Inversion

Vertical concentration profile

Averaging Kernels, DOFs, error estimates

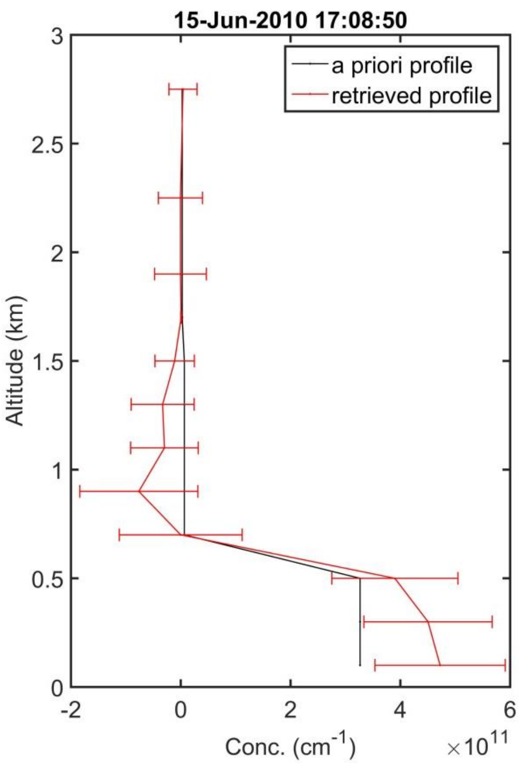

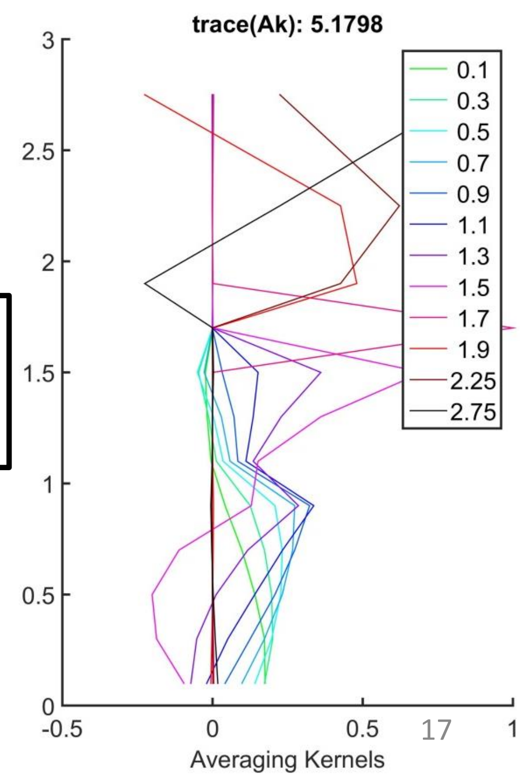

How much altitude information can we retrieve?

Approach:

- Simulate Aerosol/NO_2 Profiles for a large range of atmospheric conditions
- Use of optimal estimation to determine information content:

Averaging Kernel:

Retrieval is sensitive to the true state

Retrieval with 1% error

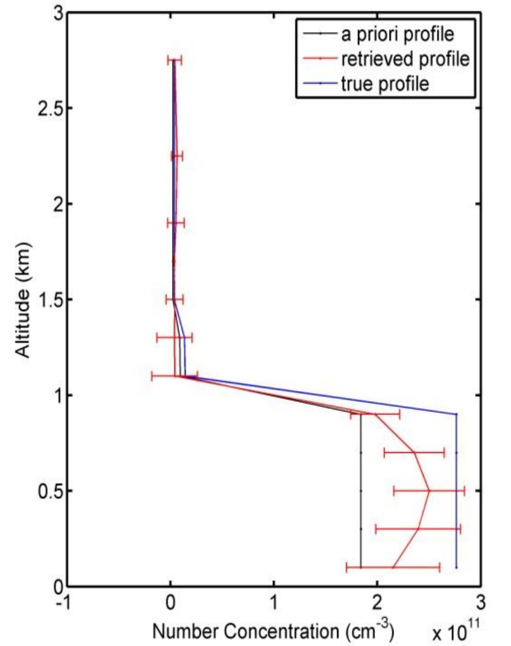

Trace(AK) = 4.5324

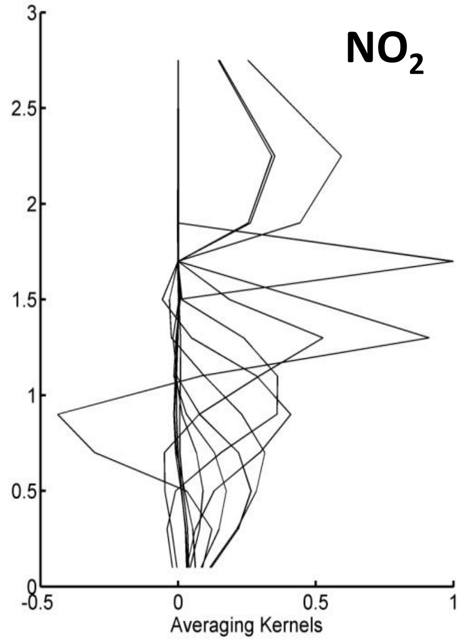

Degrees of Freedom :

Number of independent pieces of information (true height resolution).

4-5 pieces of NO_2 altitude information can be obtained from the MAX-DOAS

		NO_2 boundary layer M.R. (ppb)			
		5	**10**	**30**	**50**
Boundary Layer Height (km)	**0.5**	4.62	4.77	4.95	5.01
	1.0	4.65	4.81	5.01	5.10
	1.5	4.67	4.86	5.07	5.17

Atmospheric NO_2 Profiles

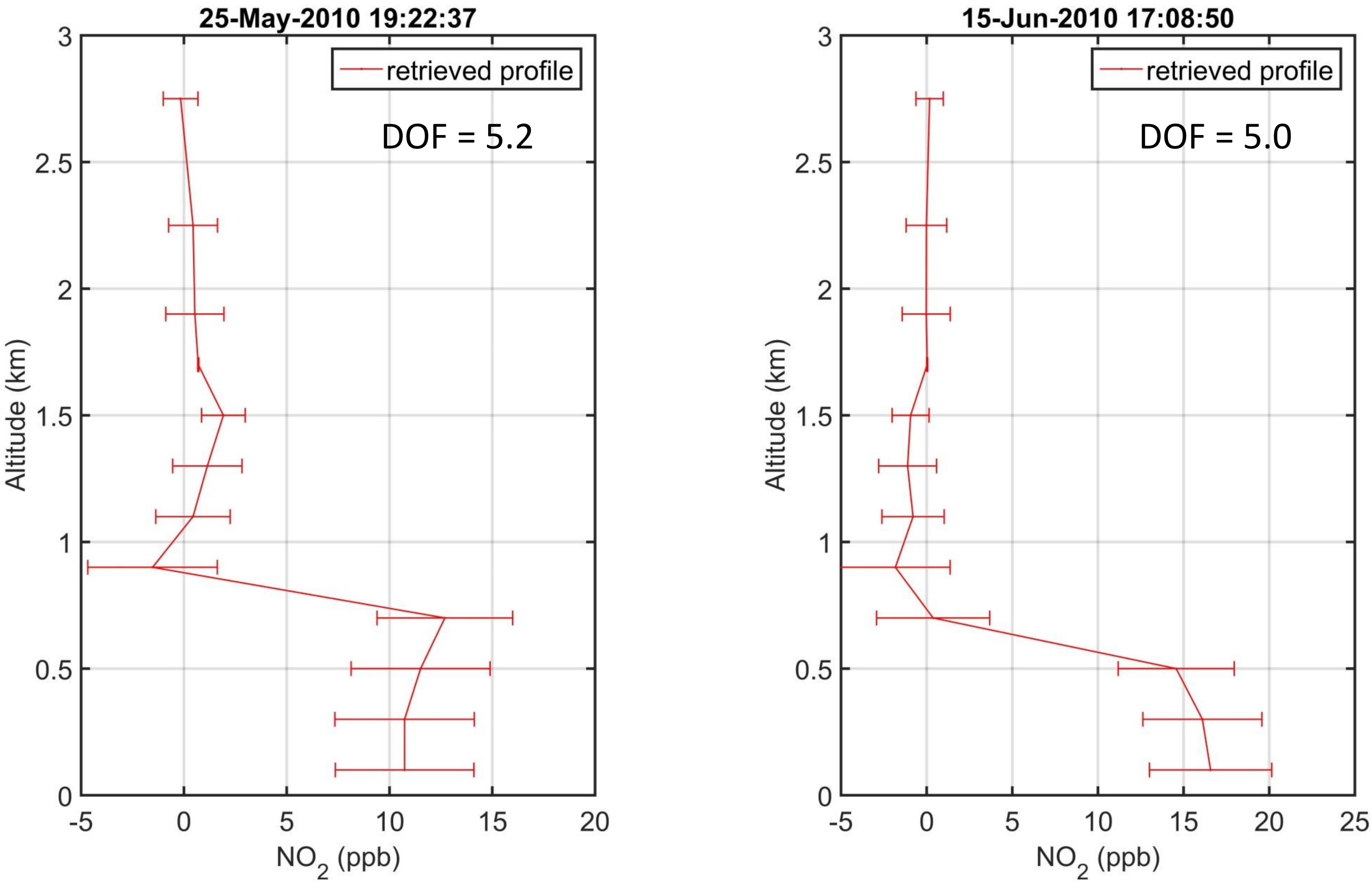

Comparison with Surface Observations

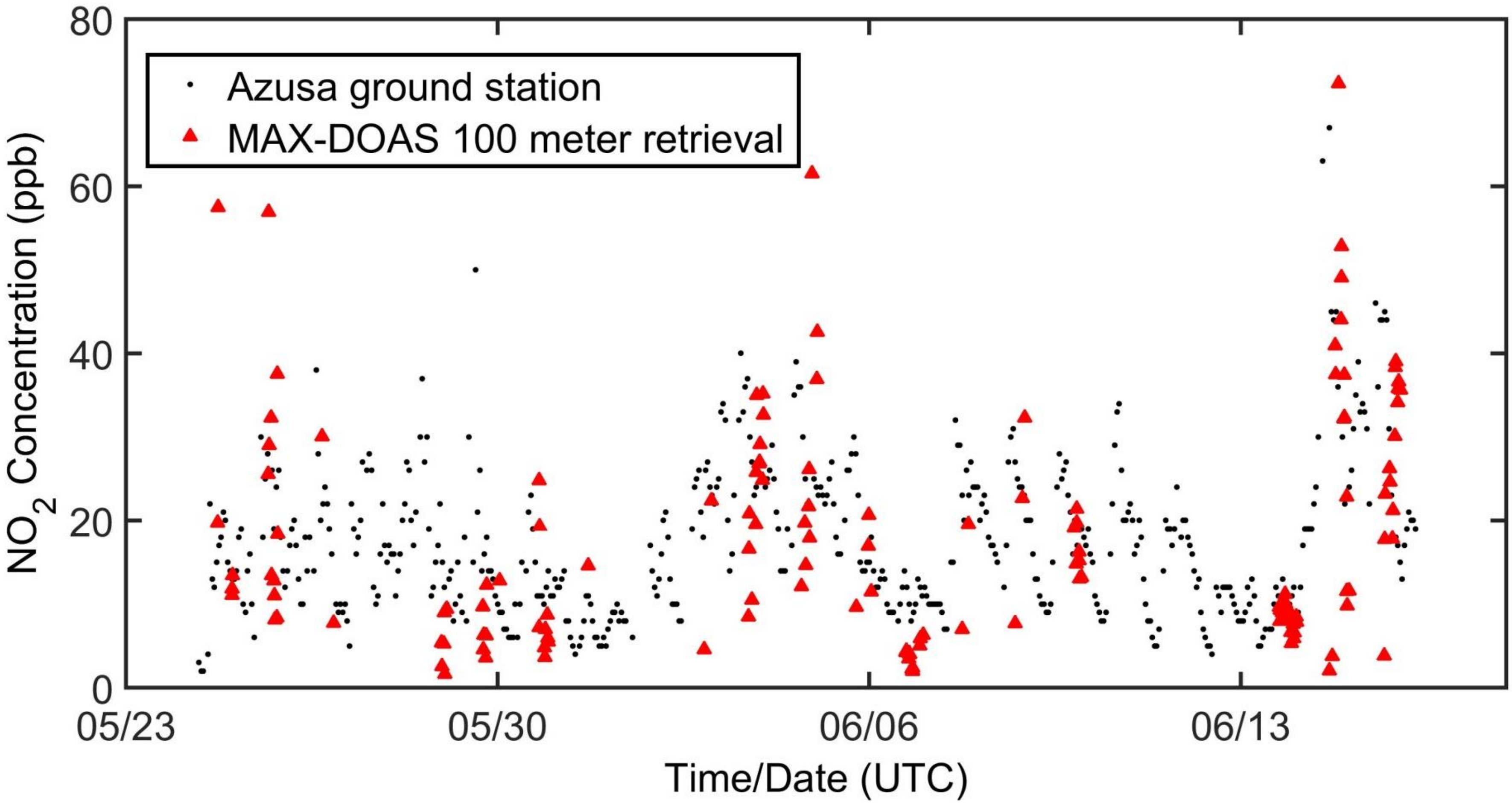

MAX-DOAS NO_2 retrieval in lowest 100m compares well with surface observations.

<u>Caveat:</u> The two instrument do not probe the same airmass!

Altitude resolved view

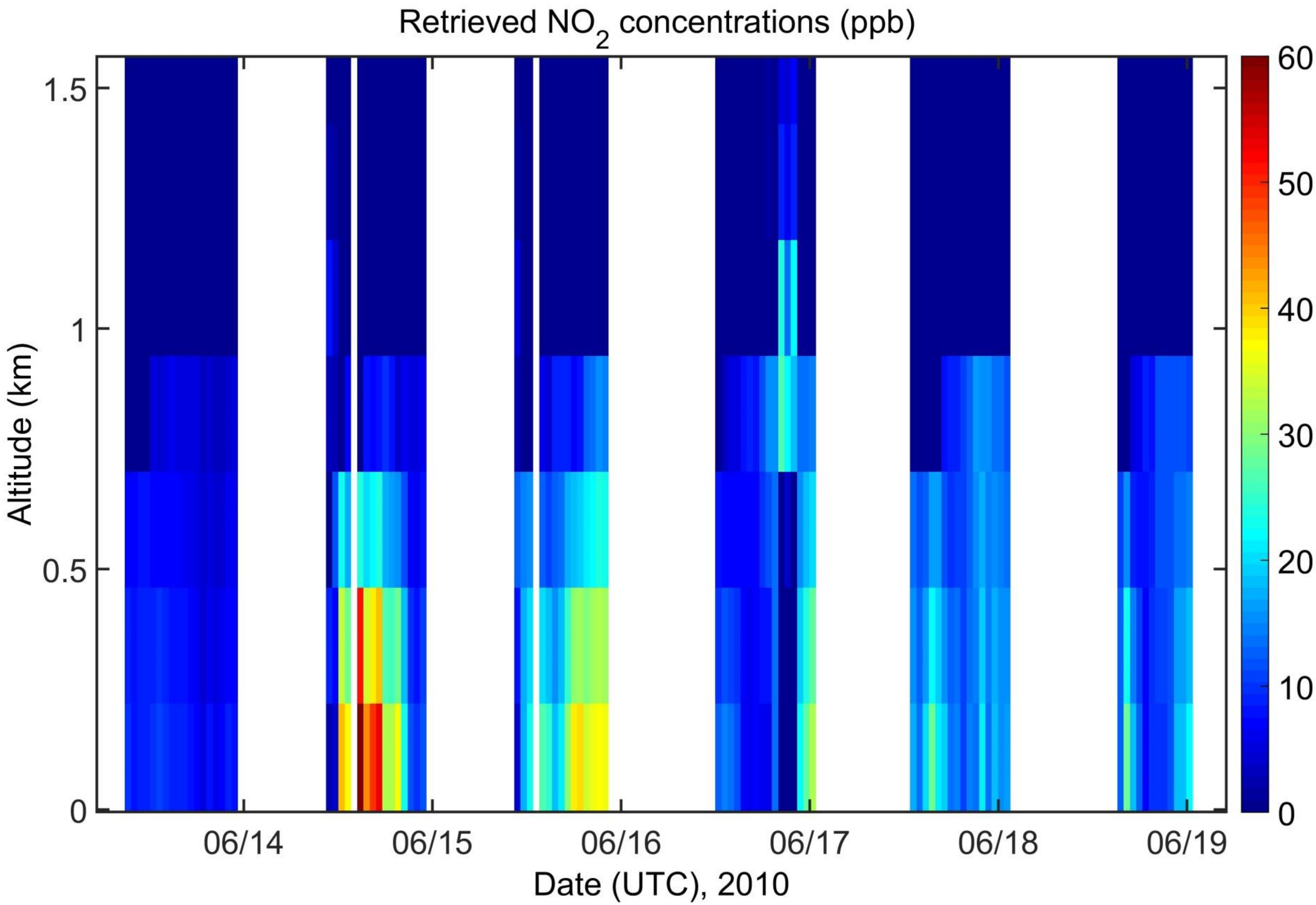

Ozone formation sensitivity from Mt. Wilson

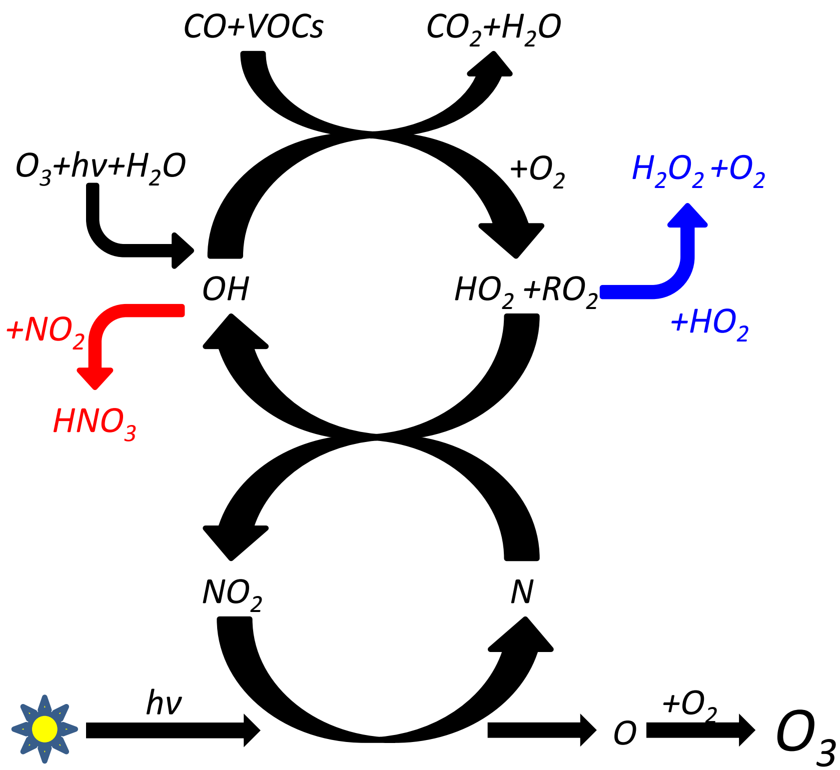

LN/Q > 0.5 VOC limited

LN/Q < 0.5 NO_x limited

Sillman et al., 1990

If L_R and L_N are the loss rates in low NO_x and high NO_x conditions, and Q is the radical production rate:

$$Q = L_R + L_N$$

Then L_N/Q is the fraction of free radicals in the atmosphere removed through reaction with NO_x

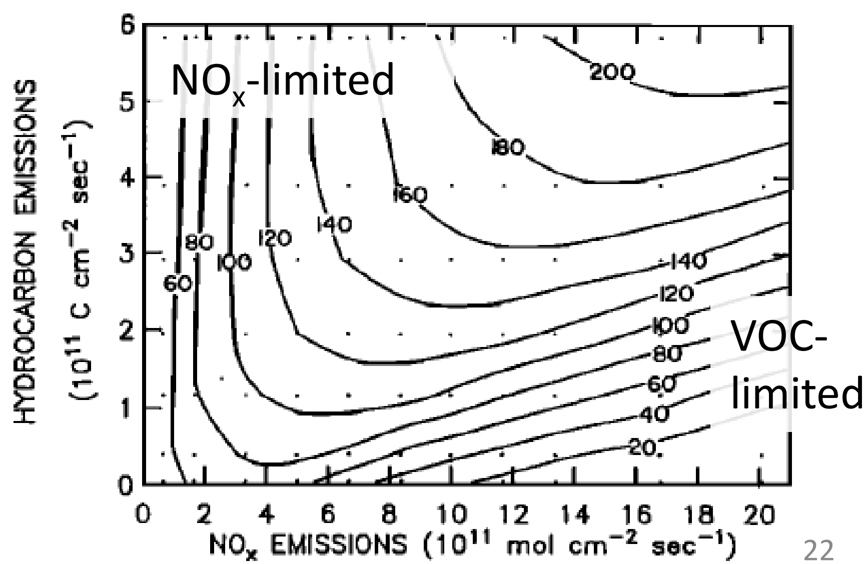

HCHO/NO_2 ratio during CalNex in Los Angeles

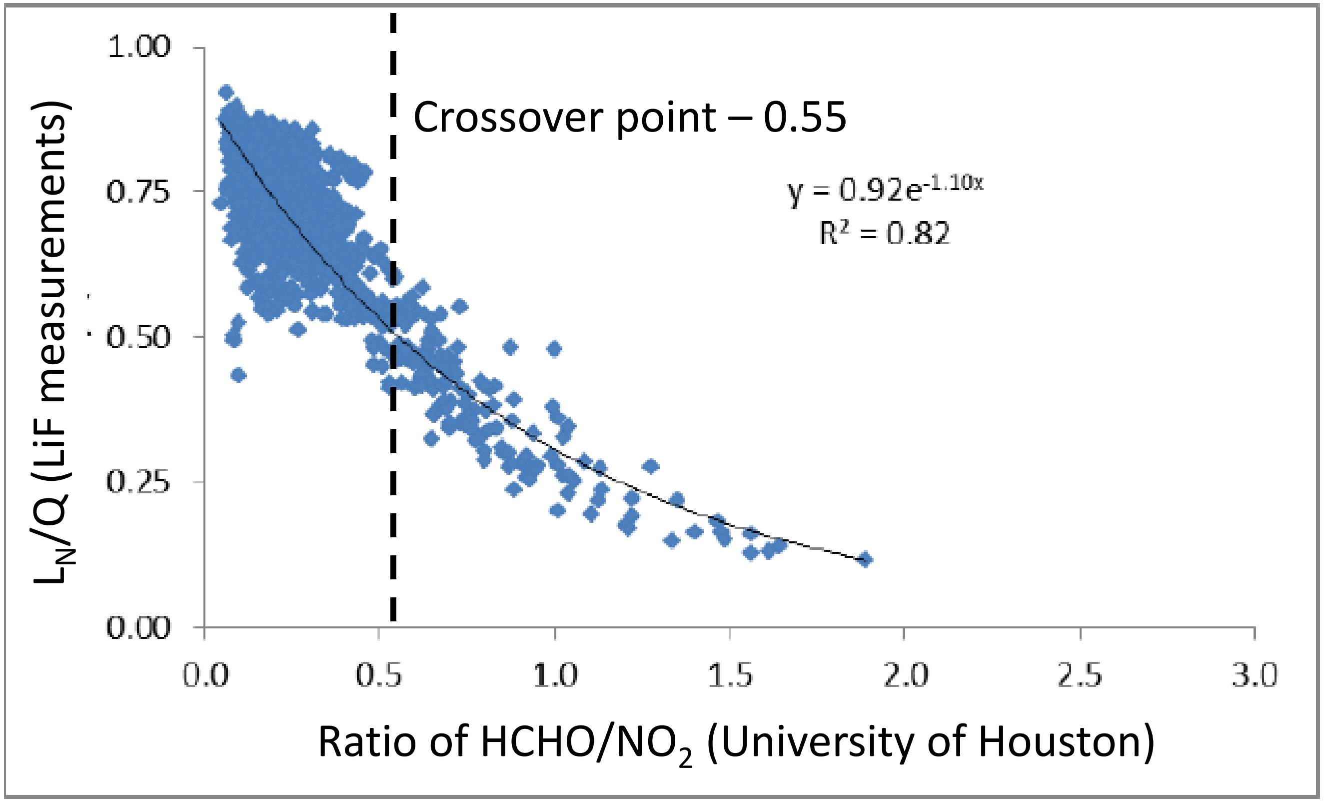

ratio < 0.55, VOC-limited regime

ratio > 0.55, NO_x-limited regime

(Ln/Q data from P. Stevens, Univ. Indiana, pers. communication, unpublished data)

HCHO/NO_2 ratio for one month

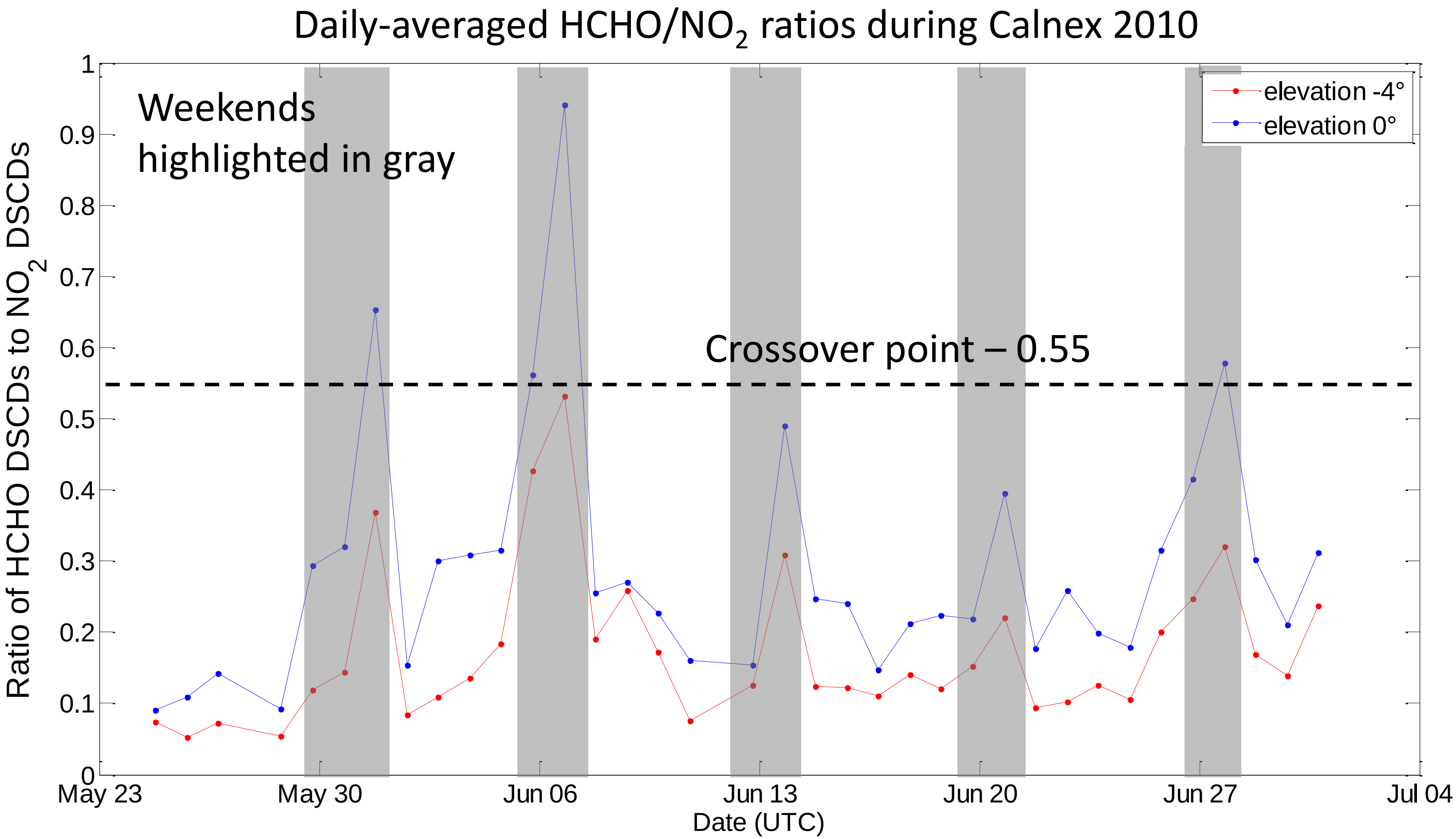

HCHO and NO_2 analyzed at same wavelength (323-350 nm) to cancel out radiative transfer effects

In agreement with higher weekend ozone in Los Angeles

Seasonal Trends in HCHO/NO_2 ratio

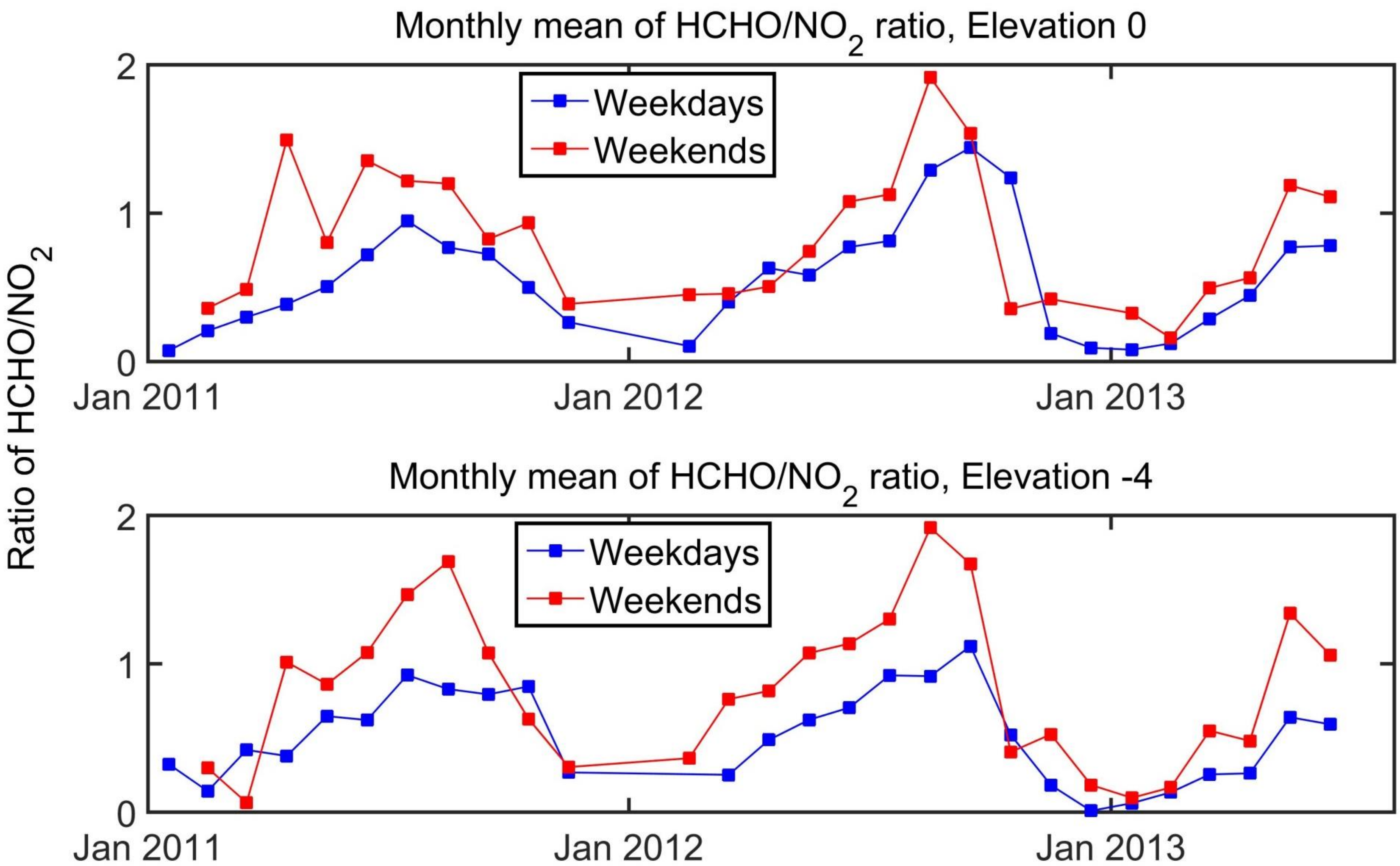

Possible explanations: reduced sunlight during winter? Greater biogenic VOC production during summer? Changes in boundary layer meteorology?

Weekend effect (observed)

Hourly-averaged DSCDs for both NO_2 and HCHO, separated by weekday and weekend. The bars show the variance.

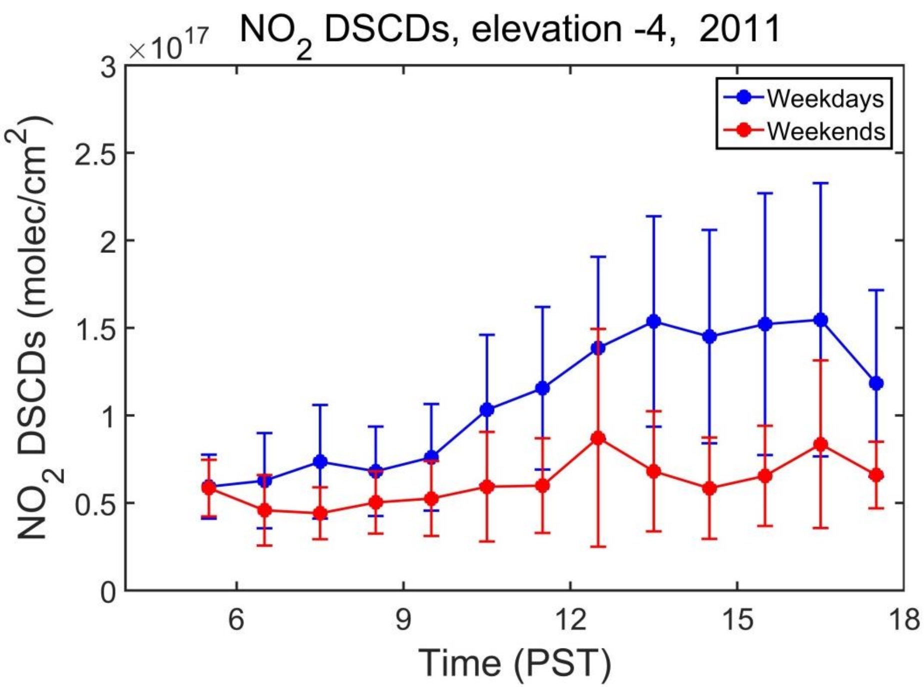

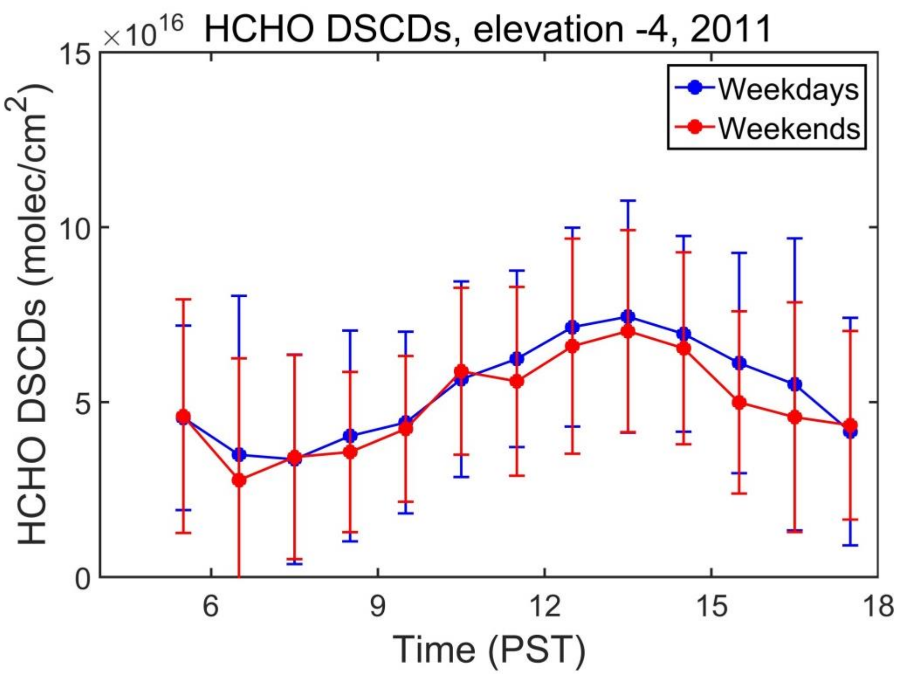

Weekend/weekday difference in ozone formation sensitivity is from NO_x concentrations / emissions

Sources of CO_2 in the LA Basin

Vehicles


Natural gas fueled power plants

- Anthropogenic CO_2 emissions primarily come from fossil fuel combustion.
- Emissions are understood to within 5-10% (California Air Resources Board, 2008)

Sources of CH_4 in the LA Basin


Wastewater treatment plants


Landfills


Dairy farms


NG Pipeline leakage

- 2^{nd} most important GHG. 25 times the global warming potential of CO_2.
- Comes from a variety of sources.
- Emissions in the LA basin have **30 to >100%** uncertainties! (Peischl et al., 2013, Jeong et al., 2013, Wunch et al., 2009; Hsu et al., 2010; Wennberg et al., 2012).
- Need to quantify emissions better!

California Laboratory for Atmospheric Remote Sensing (CLARS)

California Laboratory for Atmospheric Remote Sensing (CLARS)

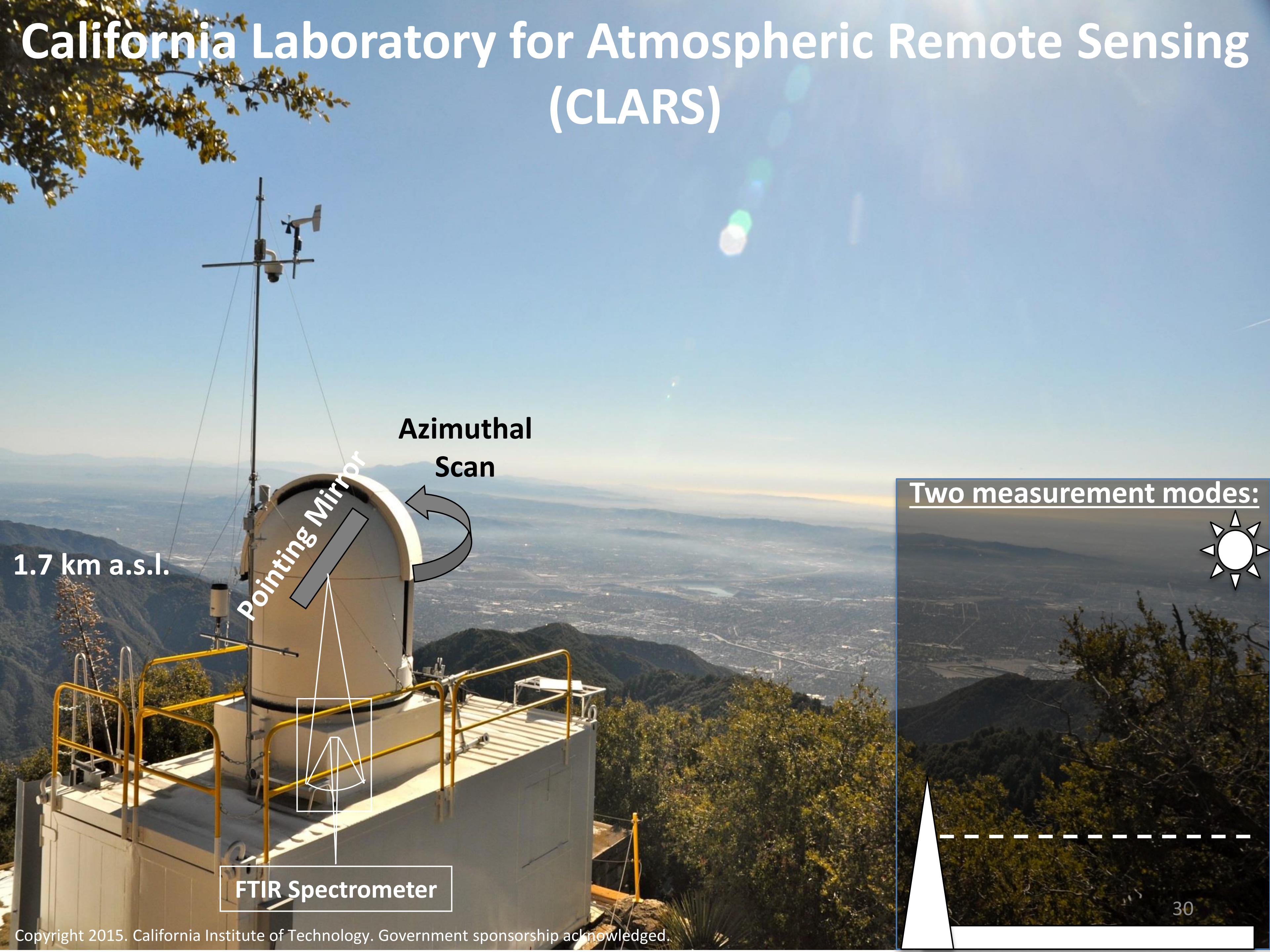

California Laboratory for Atmospheric Remote Sensing (CLARS)

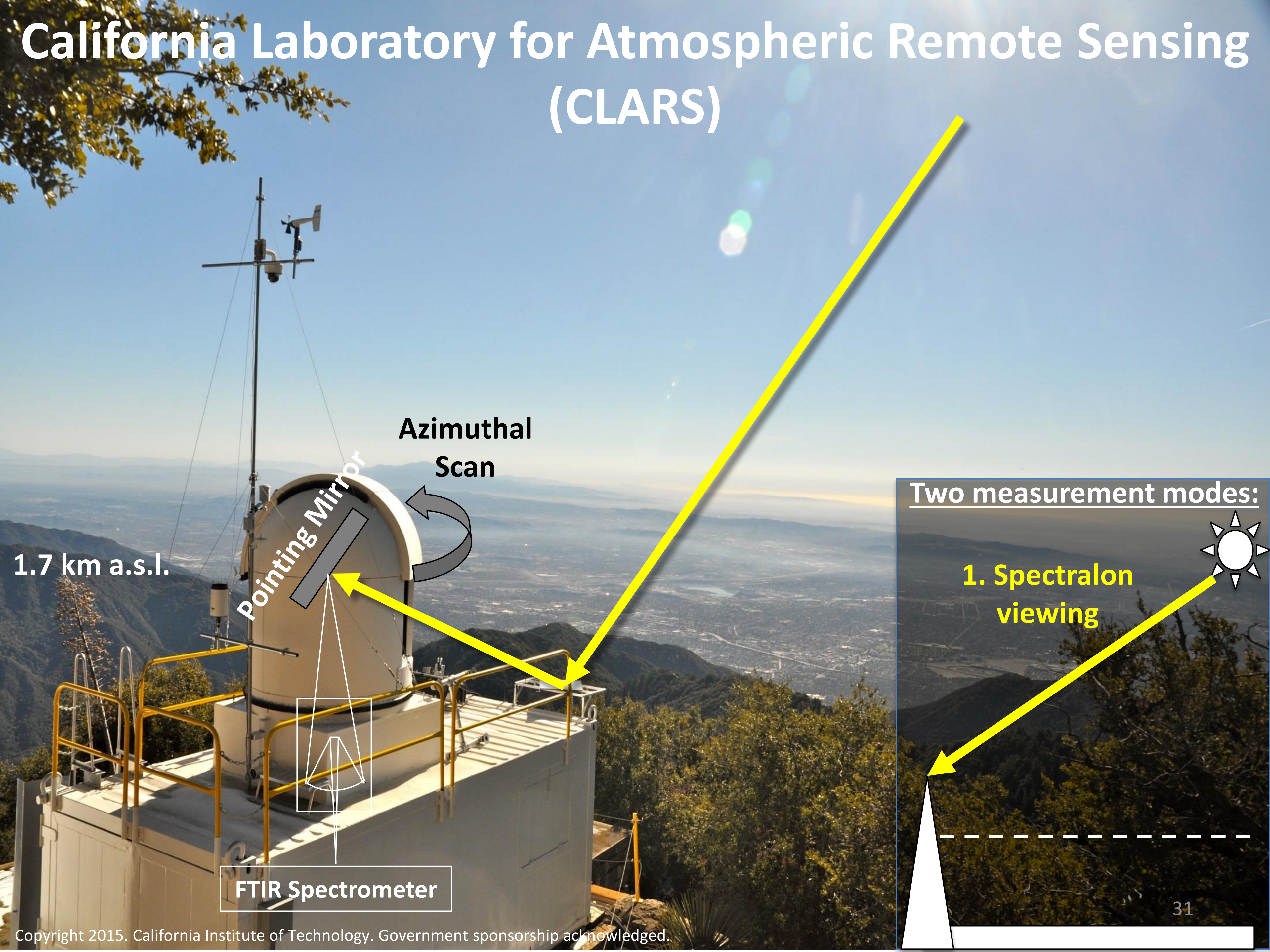

California Laboratory for Atmospheric Remote Sensing (CLARS)

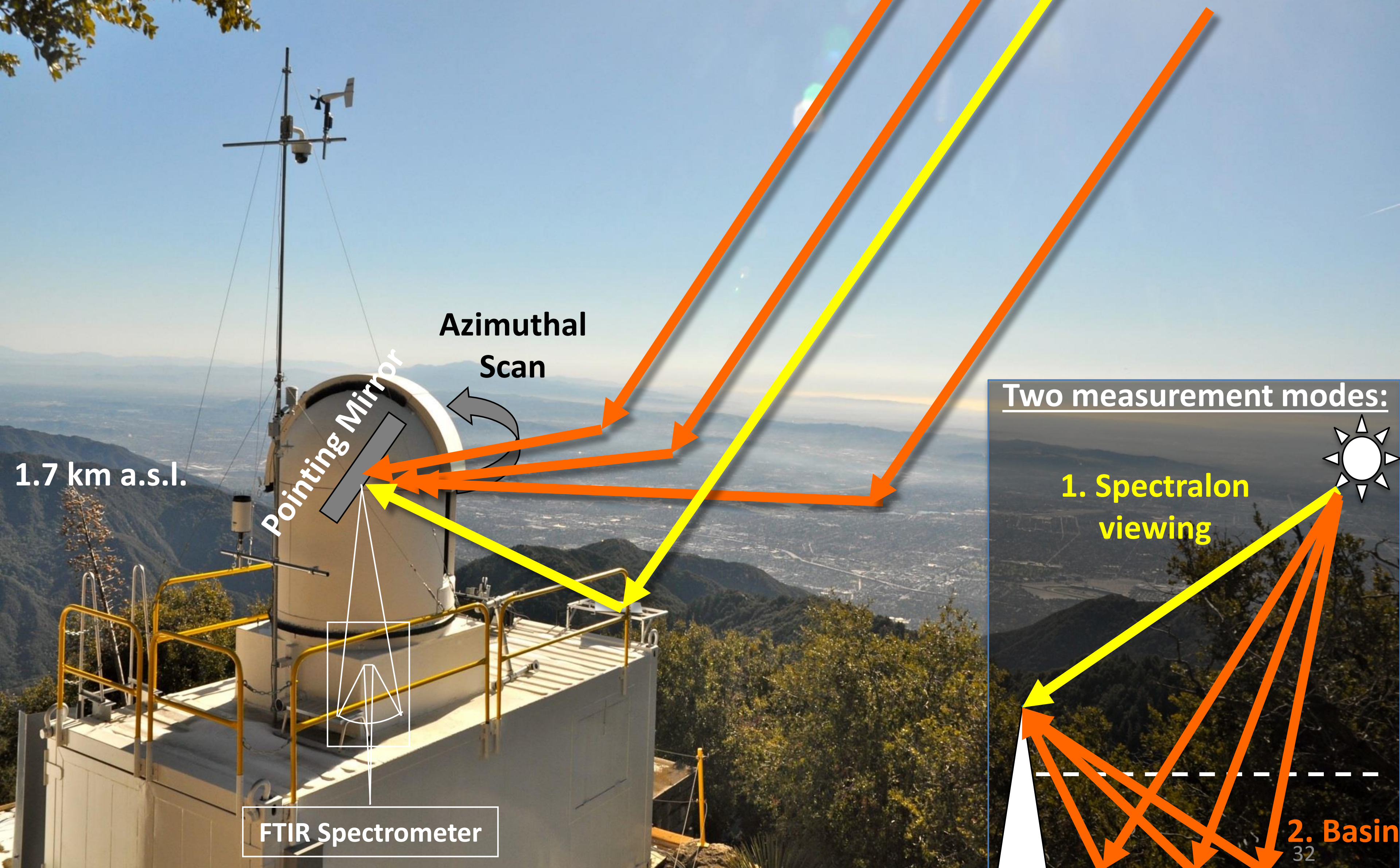

California Laboratory for Atmospheric Remote Sensing (CLARS)

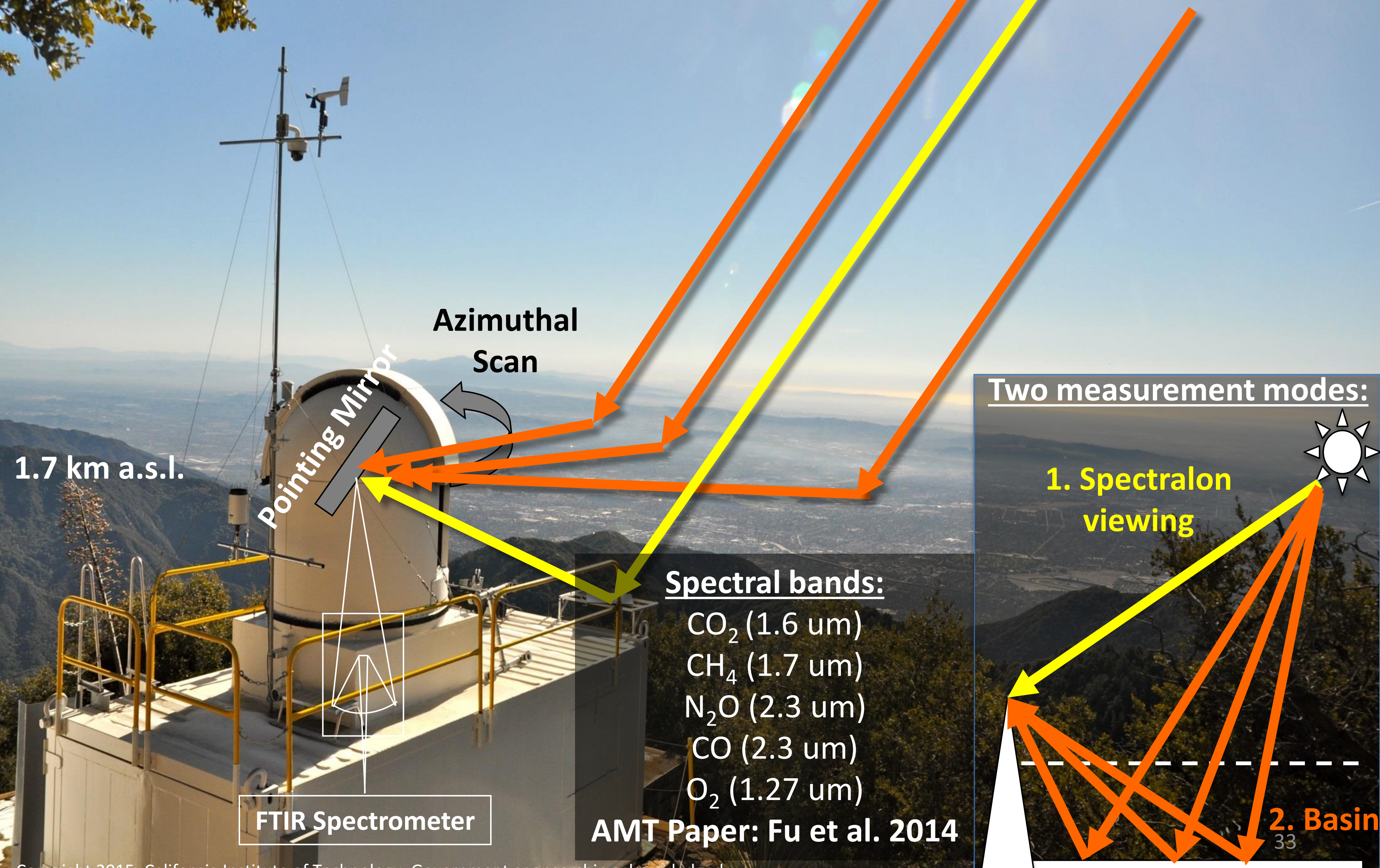

basin reflection points

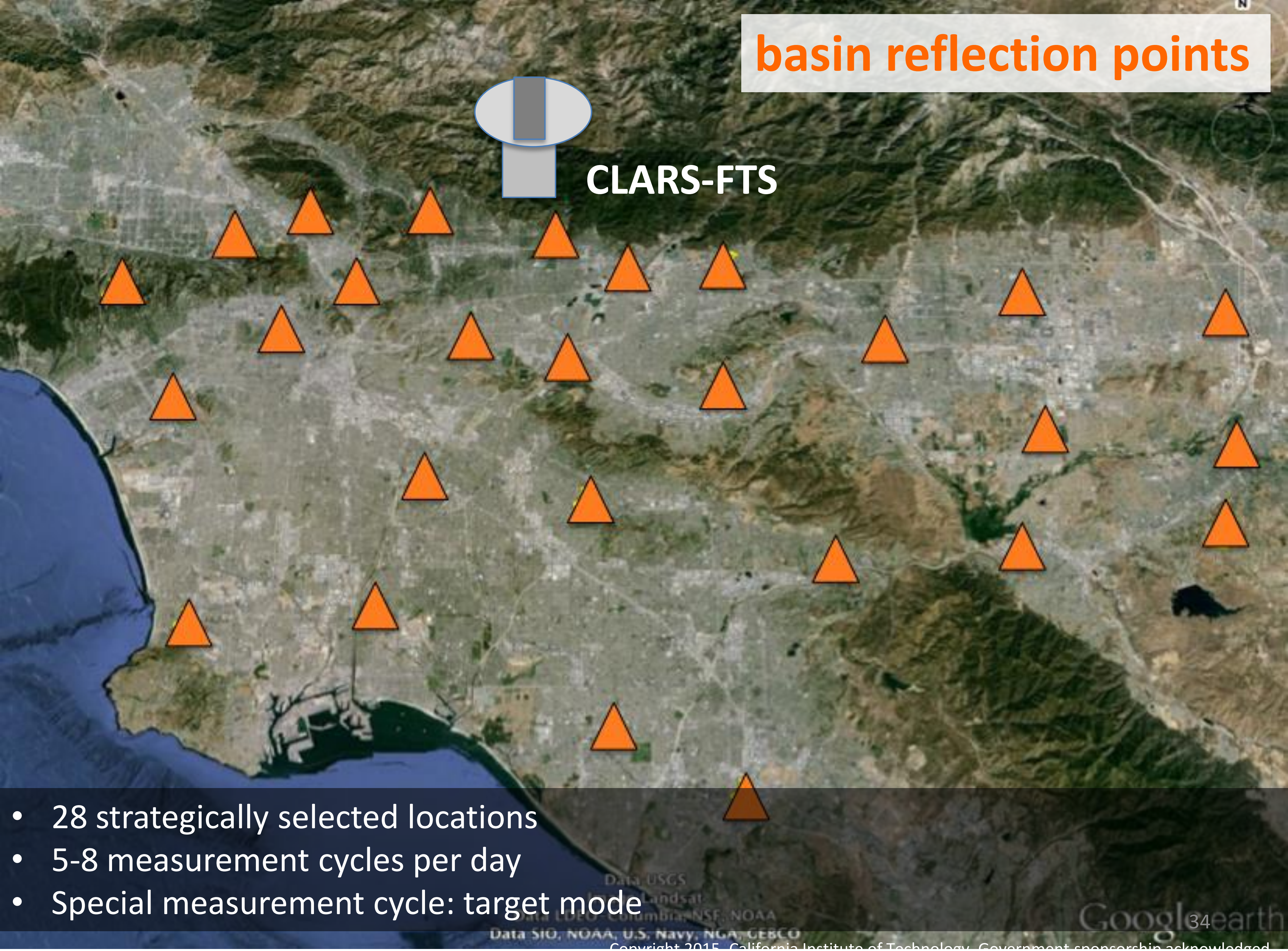

- 28 strategically selected locations
- 5-8 measurement cycles per day
- Special measurement cycle: target mode

Diurnal patterns of XCO_2 and XCH_4

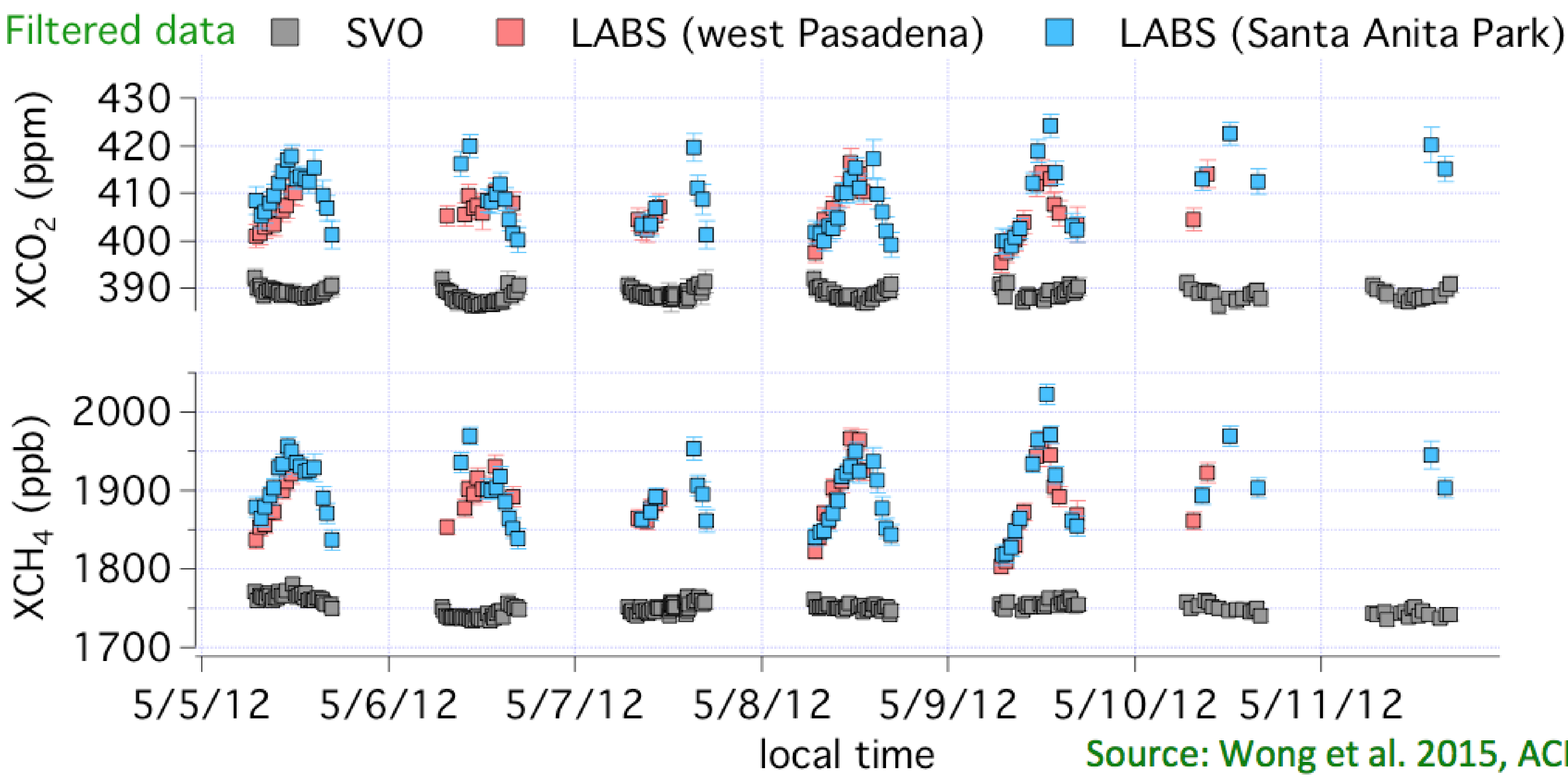

Source: Wong et al. 2015, ACP

Correlations between $XCH_{4(xs)}$ and $XCO_{2(xs)}$

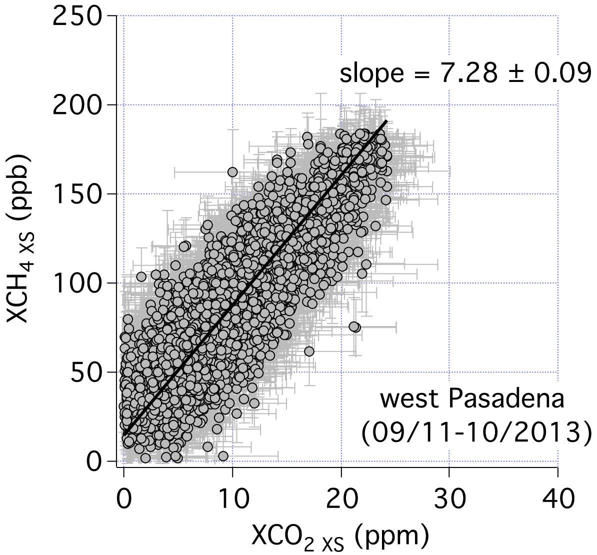

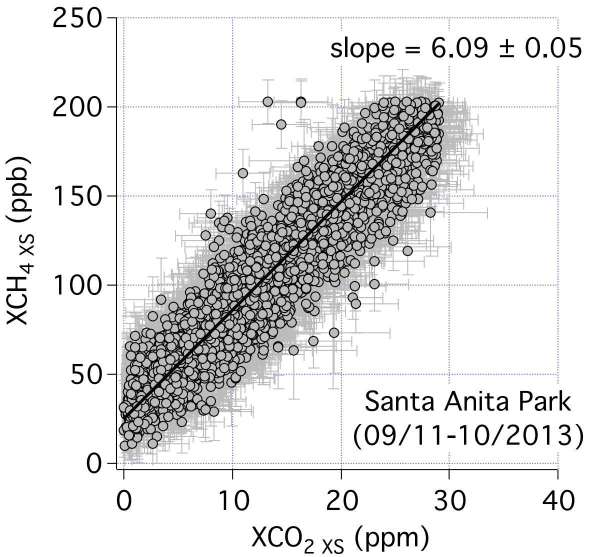

- Tight correlations were observed between XCH_4 and XCO_2 excess mixing ratios.
- The correlation slopes indicate the relative emission flux of the two GHGs in Los Angeles.

Correlations between $XCH_{4(xs)}$ and $XCO_{2(xs)}$

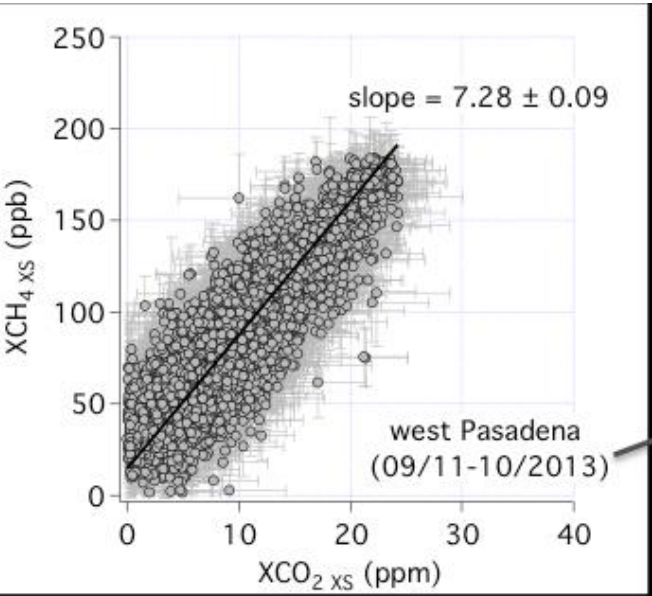

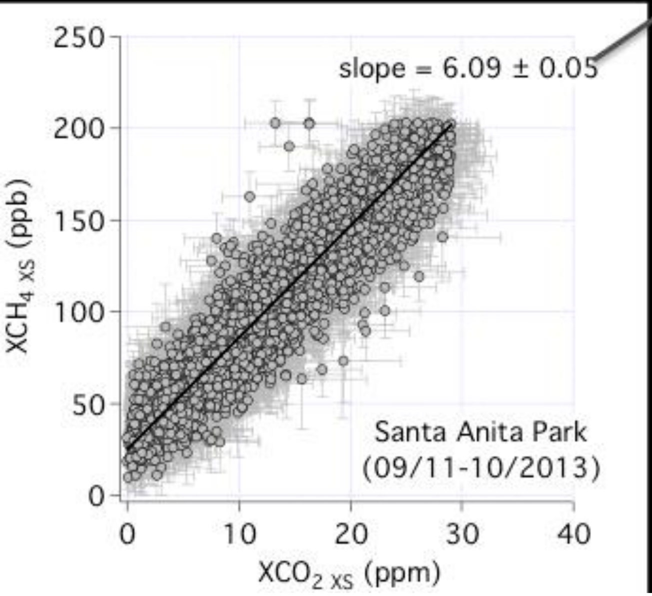

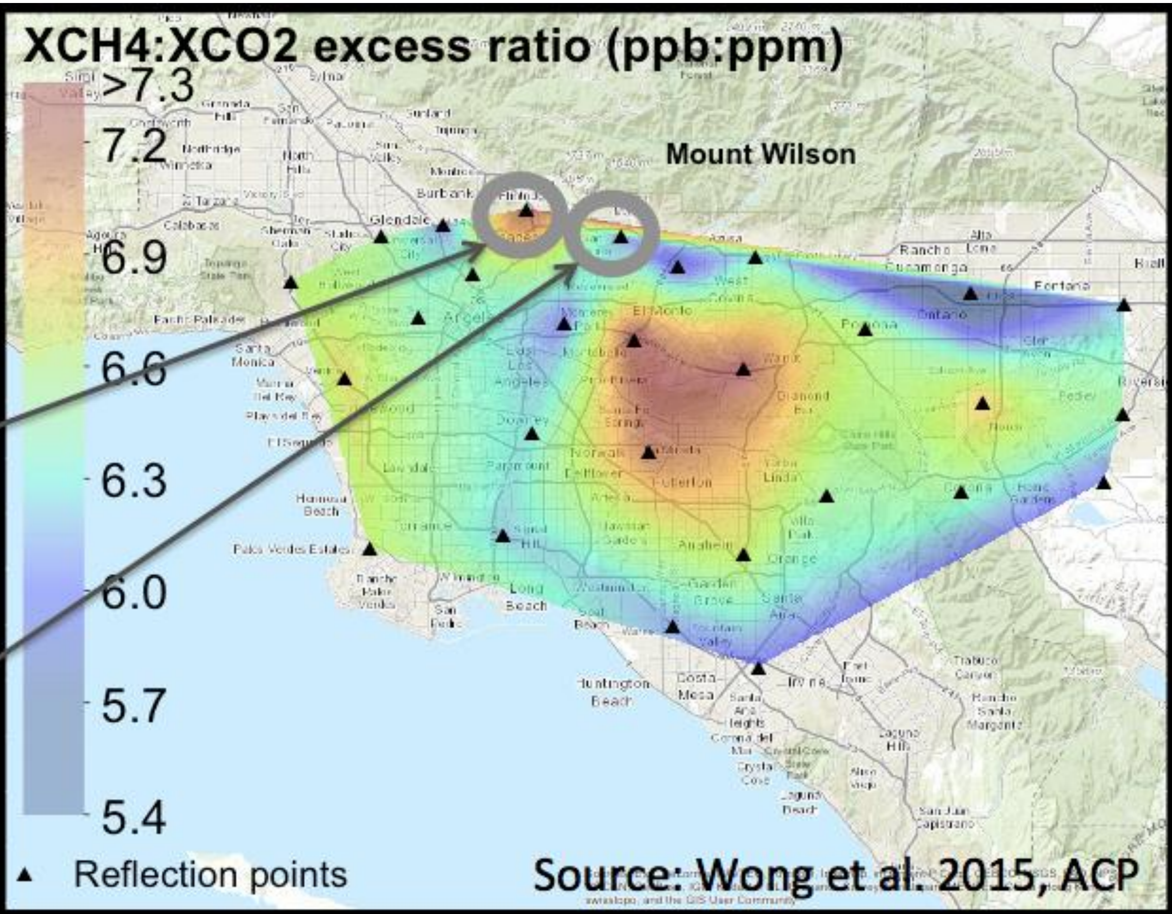

- Spatial averaging causes smearing of plumes, making attribution of point sources difficult without knowing atmospheric transport.
- This can be improved in the further when the observations are integrated with an atmospheric transport model.

Derived CH_4 Flux in Los Angeles

$$\text{Derived } CH_4 \text{ emission} = CO_2 \text{ emission} \times \frac{CH_4}{CO_2}\Big|_{\text{observed}} \times \frac{MW_{CH_4}}{MW_{CO_2}}$$

- Derived CH_4 emission is 0.39 ± 0.06 Tg CH_4/year.

Comparison with Previous Studies

Measurement (Location, period)	$CH_4 : CO_2$ ratio (ppb:ppm)	Derived top-down CH_4 emission ($Tg\,CH_4\,year^{-1}$)	Measurement type	References
TCCON (Pasadena, Aug 2007–Jun 2008)	7.80 ± 0.80	0.40 ± 0.10 0.60 ± 0.10	Column (FTS)	Wunch et al. (2009)
ARCTAS (LA, Jun 2008)	6.74 ± 0.58	0.47 ± 0.10	Aircraft in-situ (Picarro)	Wennberg et al. (2012)
CalNex (LA, May 2010–Jun 2010)	6.70 ± 0.01	0.41 ± 0.04	Aircraft in-situ (Picarro)	Peischl et al. (2013)
Caltech (Pasadena, Feb 2012–Aug 2012)	6.30 ± 0.01	0.38 ± 0.05	Surface in-situ	Newman and Hsu, per. comm. (2014)
Mount Wilson (Pasadena, Sep 2011–Jun 2013)	6.10 ± 0.10	0.37 ± 0.05	Surface in-situ (Picarro)	Hsu, per comm. (2014)
CLARS-FTS, Mount Wilson (LA, Sep 2011–Oct 2013)	6.40 ± 0.50	0.39 ± 0.06	Column (FTS)	This study

- Results are consistent with previous studies.

Monthly Spatial Distribution in CH_4:CO_2

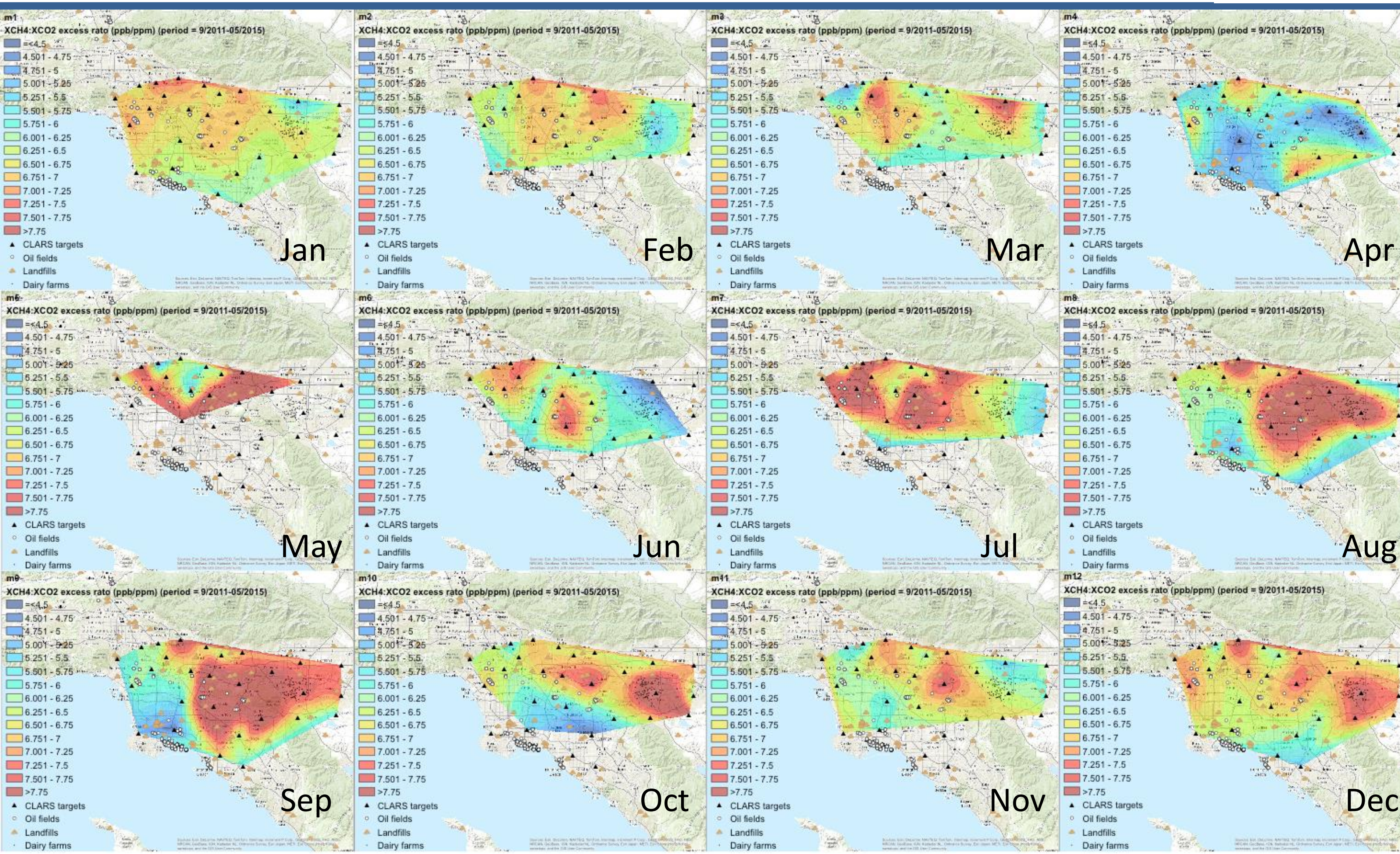

Monthly CH_4:CO_2 Trend in Los Angeles Basin

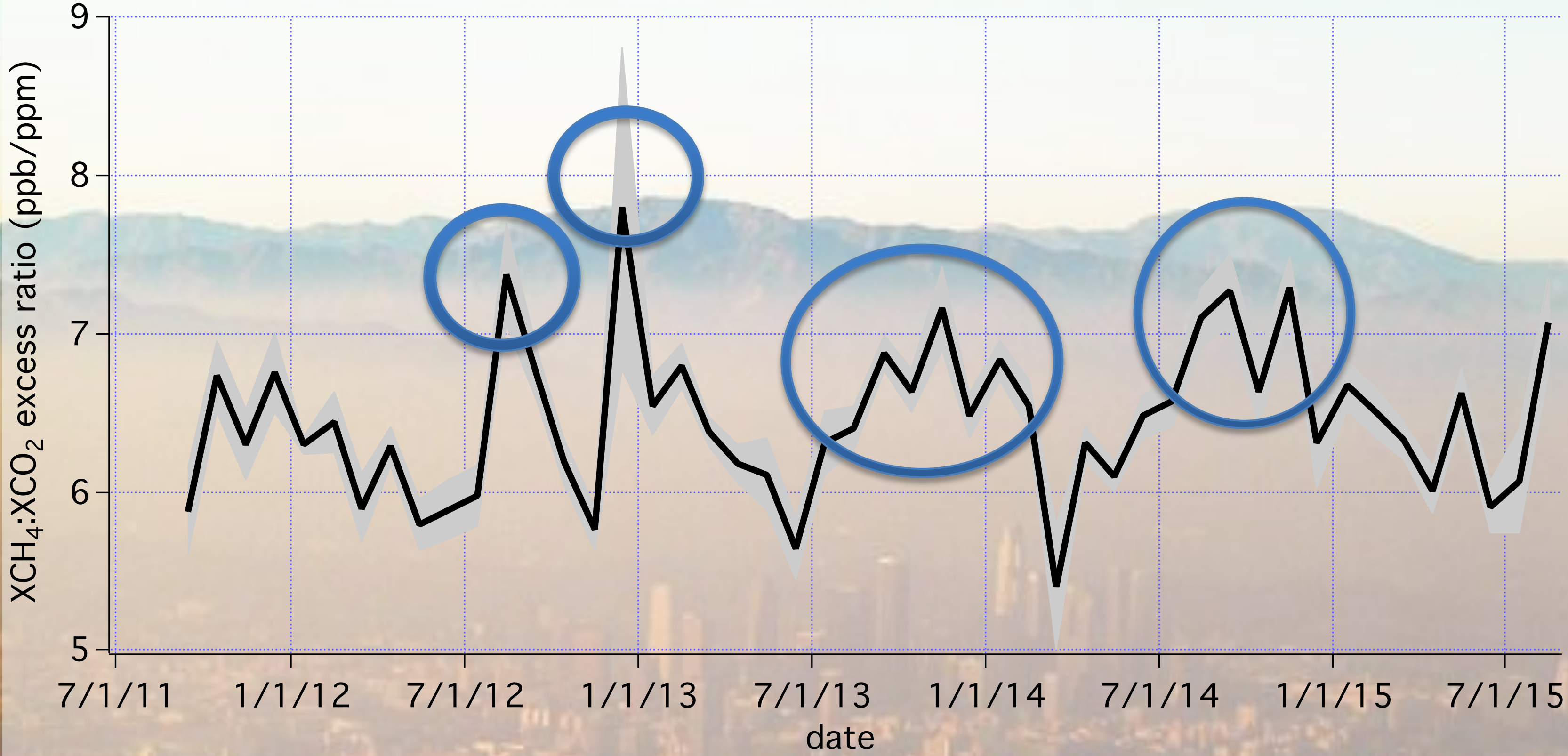

- CH_4:CO_2 ratio shows 20-28% seasonal cycle with peaks in fall and winter.

Monthly Top-Down Total CH_4 Emission Trend

Courtesy to K. Gurney (ASU) for Hestia data.

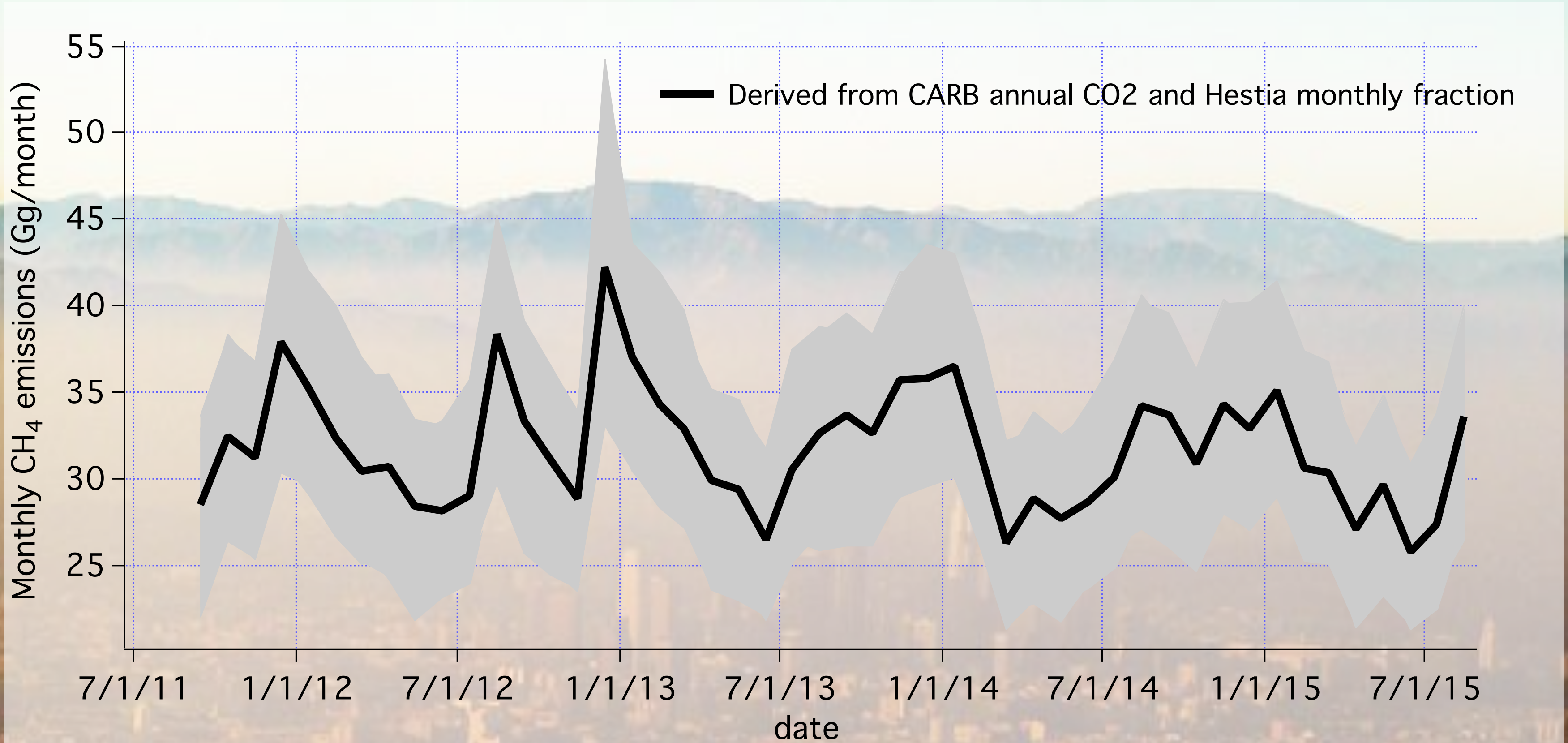

- Derived top-down methane emissions show consistent peaks in fall and winter in the basin.

Annual Trend in CH_4 emissions

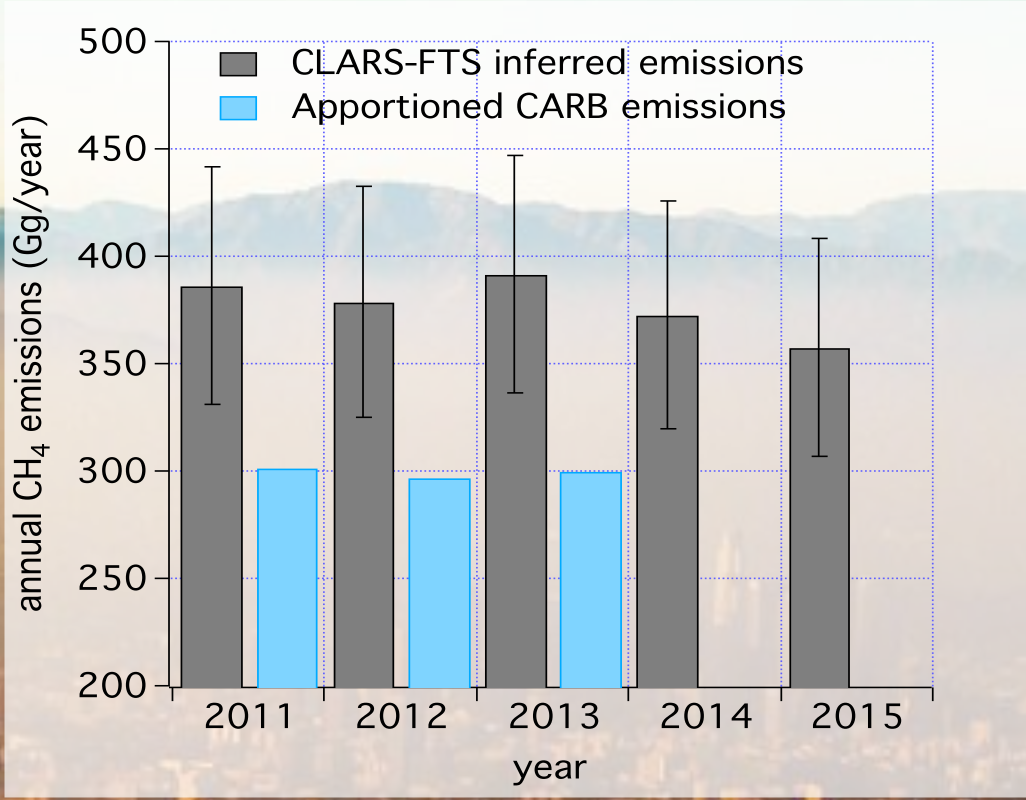

- Little interannual trends were observed from 2011 to 2015.
- Derived emissions are significantly larger than the bottom-up emission inventory.

More than 130 families relocated after methane leak near Porter Ranch

This Nov. 3 photo provided by Southern California Gas Co. shows equipment being used as crews and technical experts try to stop the flow of natural gas leaking from a storage well at the utility's Aliso Canyon facility. (Javier Mendoza / Associated Press)

Mapping CH_4:CO_2 During Aliso Canyon Gas Leak

Prior to leak

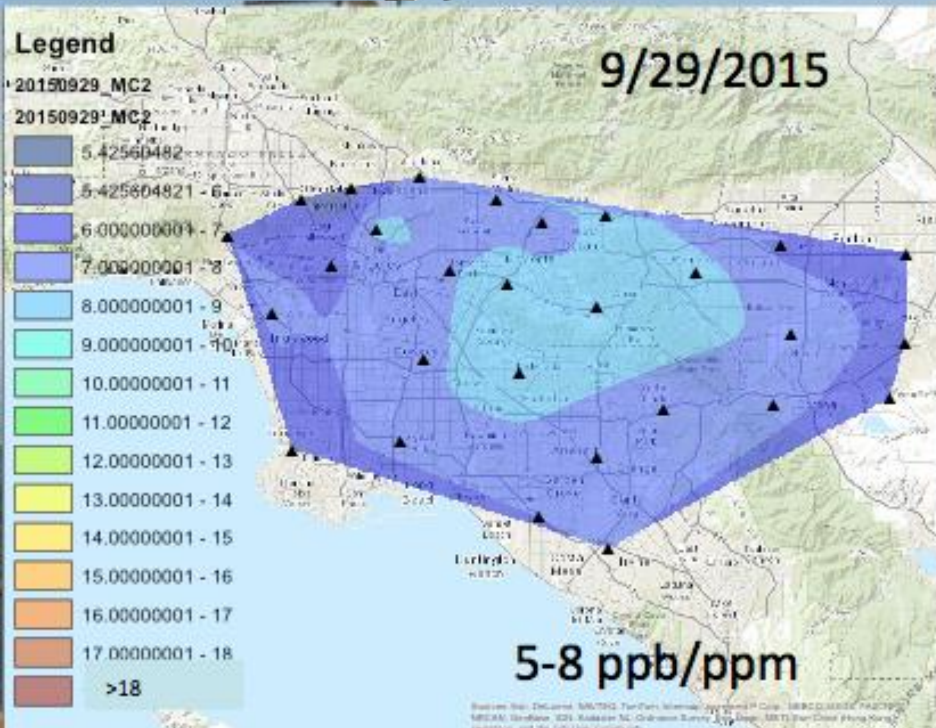

Leak in progress

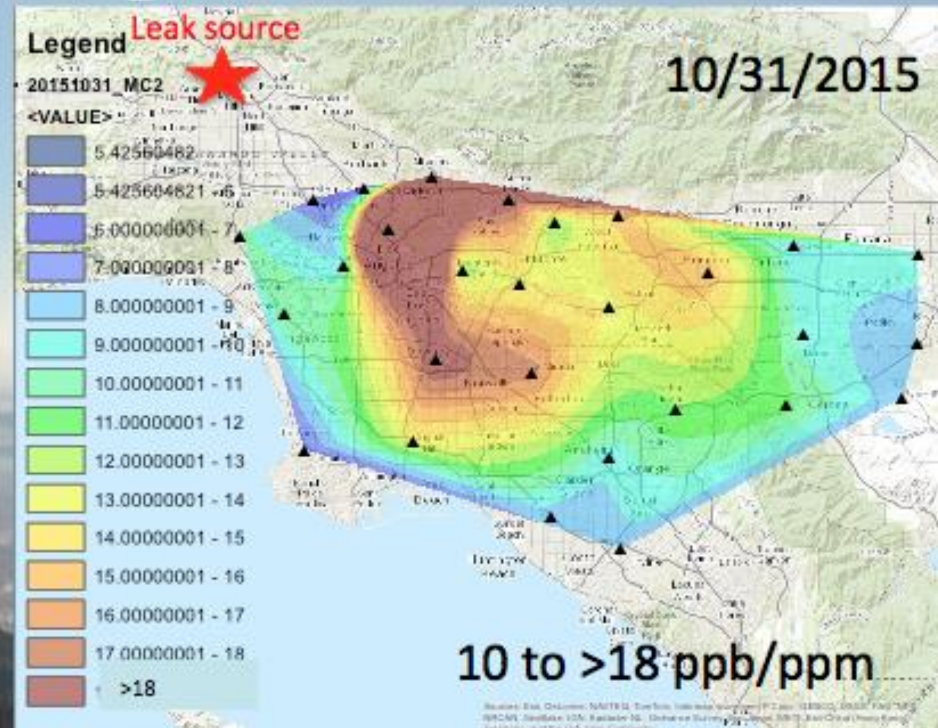

- CLARS-FTS maps significantly larger CH_4:CO_2 ratios during the leak.
- Further analysis is necessary to derive a flux from the gas leak.

Conclusions

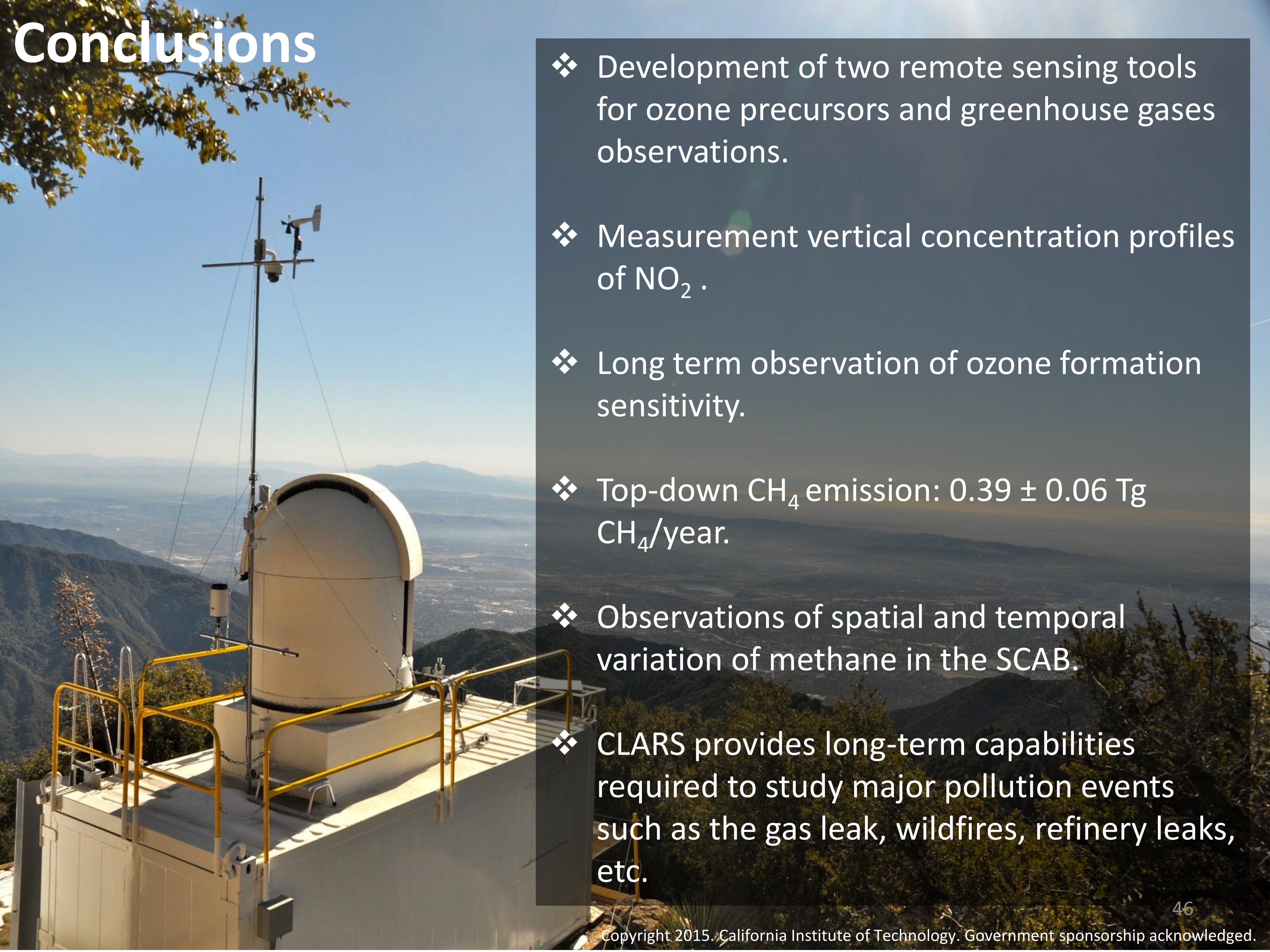

- Development of two remote sensing tools for ozone precursors and greenhouse gases observations.
- Measurement vertical concentration profiles of NO_2 .
- Long term observation of ozone formation sensitivity.
- Top-down CH_4 emission: 0.39 ± 0.06 Tg CH_4/year.
- Observations of spatial and temporal variation of methane in the SCAB.
- CLARS provides long-term capabilities required to study major pollution events such as the gas leak, wildfires, refinery leaks, etc.

Future work:

- Optimize vertical aerosol extinction profile retrievals.
- Investigation of seasonal cycle of HCHO/NO_2 ratio and ozone formation sensitivity.
- Investigating seasonal cycles of CH_4 emissions from various sources.
- Investigating the role of transport in seasonal monthly CH_4:CO_2 spatial patterns in the basin.
- Combining CLARS observations with model to derive and track spatio-temporal GHG fluxes in the Los Angeles basin.

Acknowledgements

Vijay Natraj from Caltech/JPL
Stephen C. Hurlock, UCLA

<u>Funding:</u>
CARB
NOAA
NASA
JPL

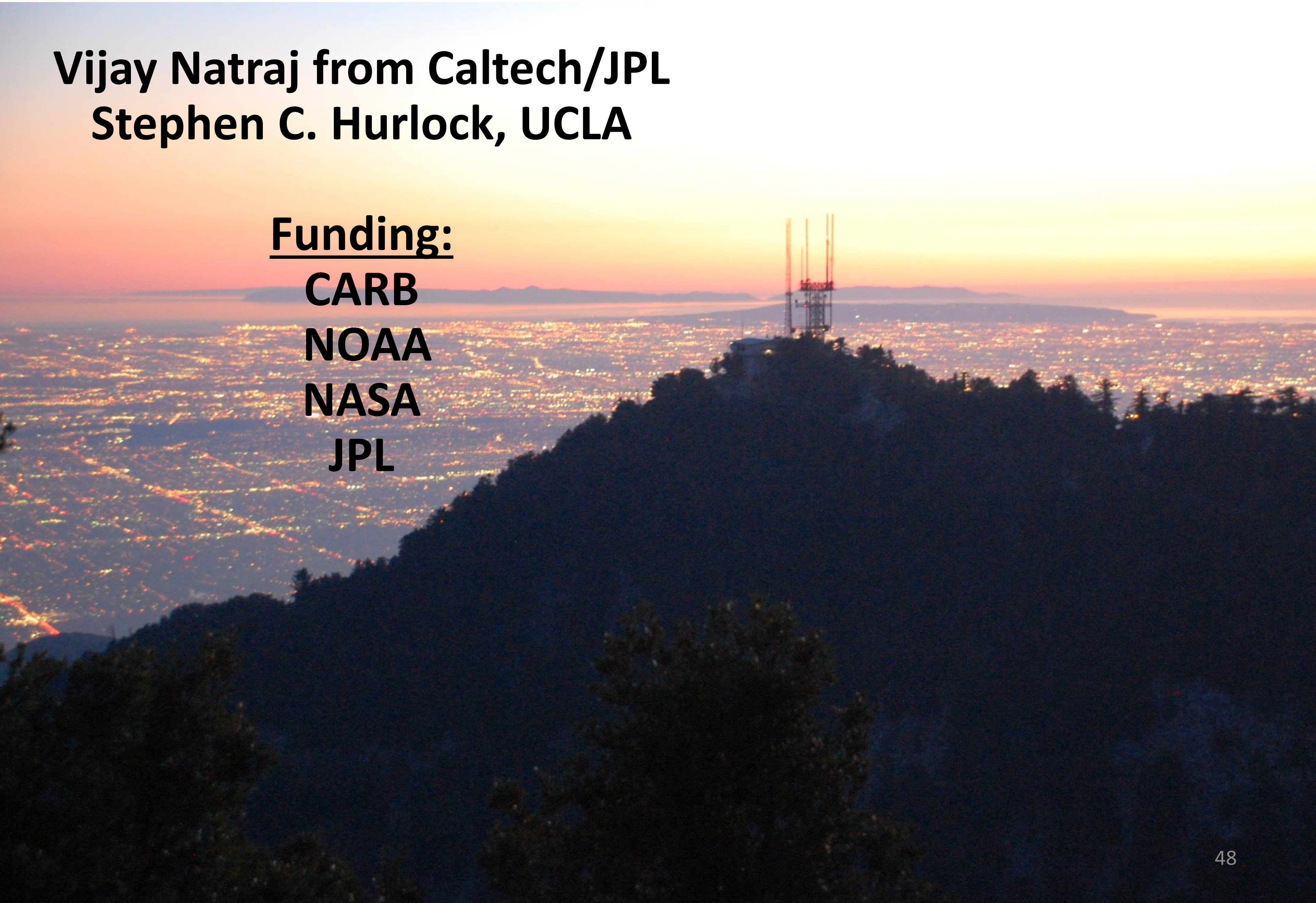

Supplemental slides

CLARS vs. WRF-VPRM CO_2 slant column

CLARS:

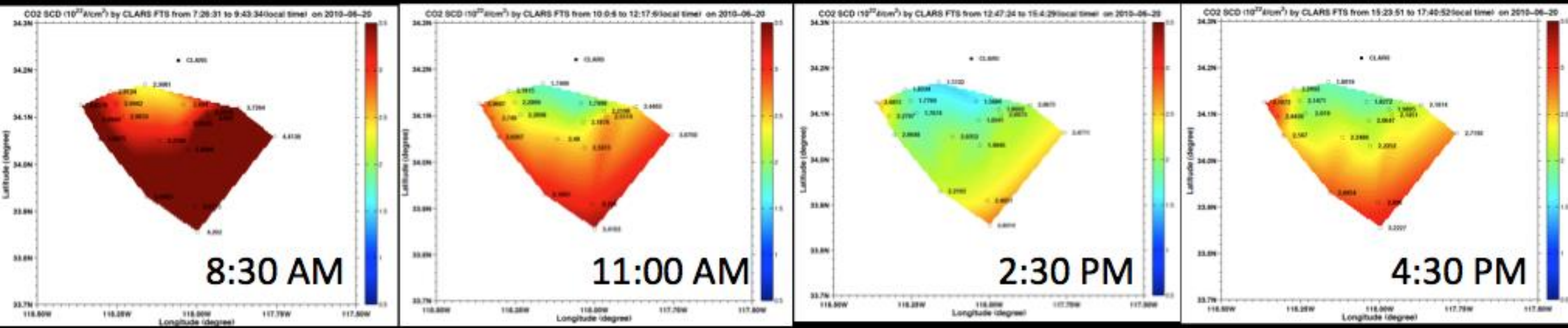

VPRM:

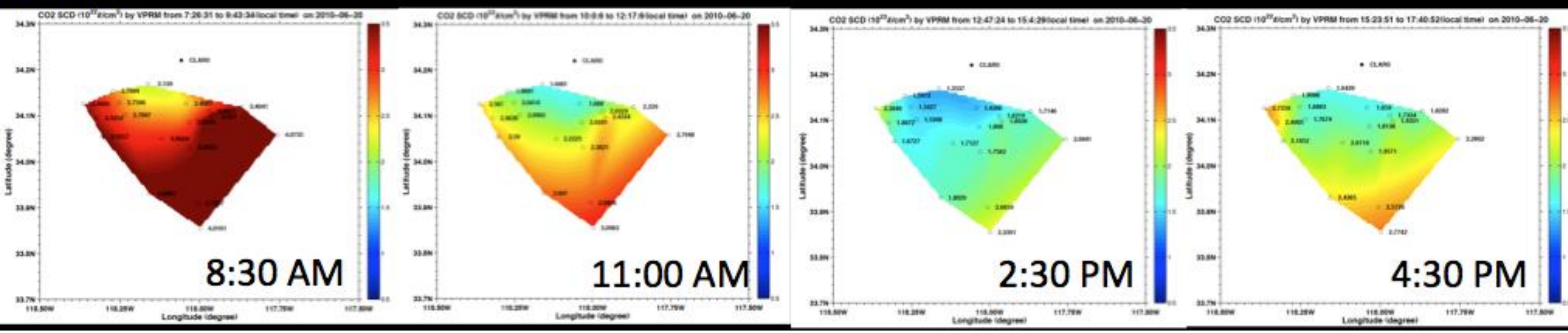

CLARS vs. WRF-VPRM CO_2 slant column

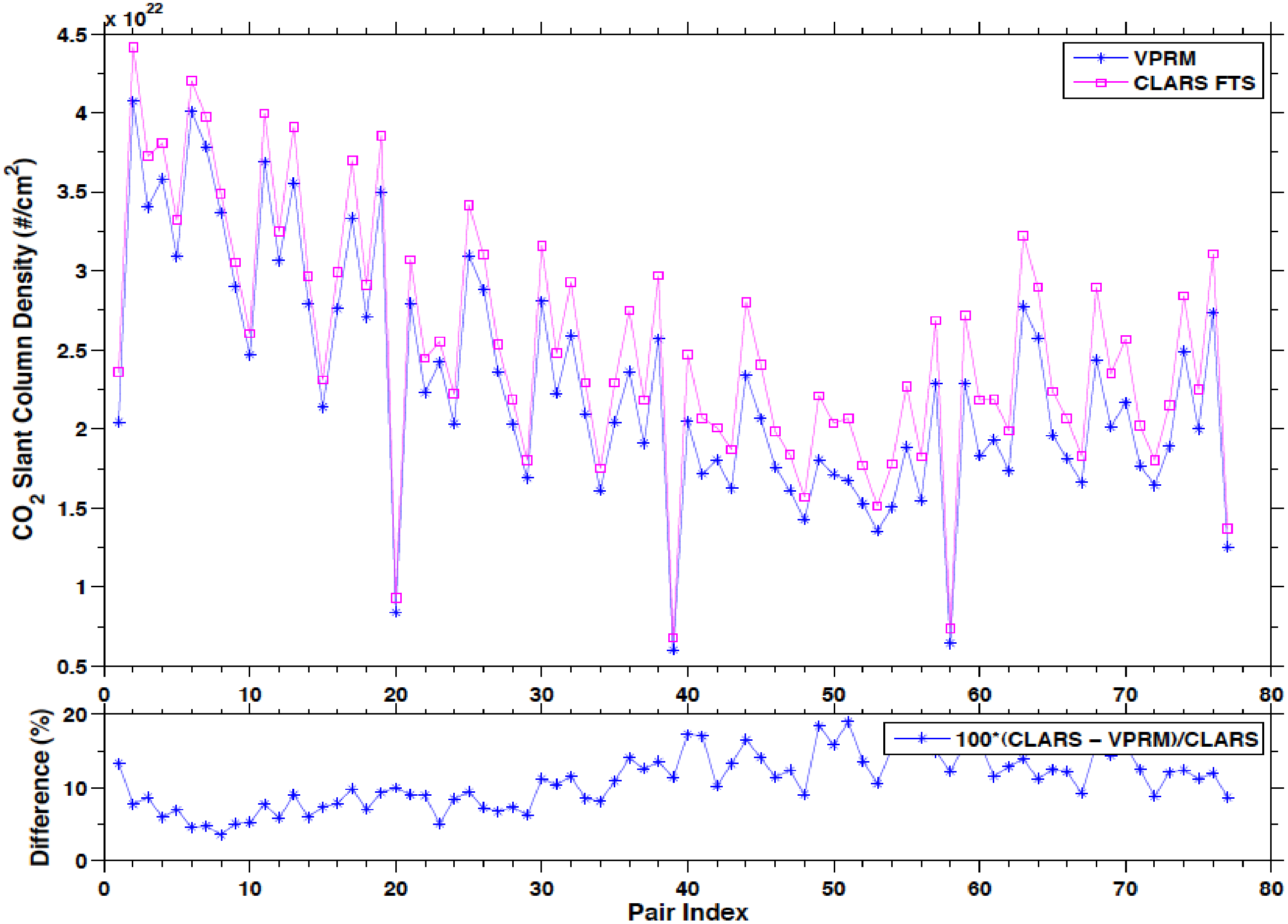

NO_2 retrievals by wavelength

DSCD: (5.3 ± 0.3) x 10^{16}

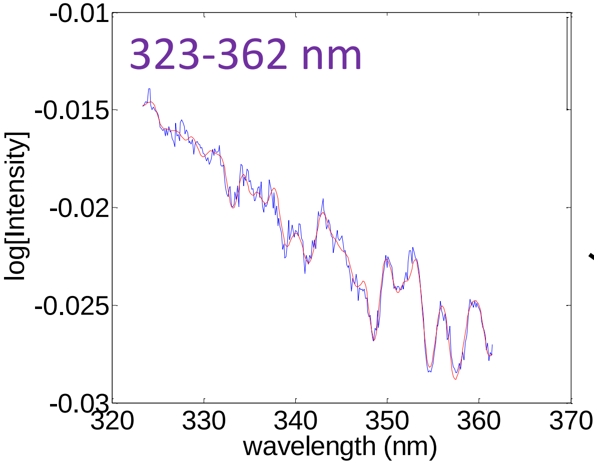

All figures are in the same viewing direction

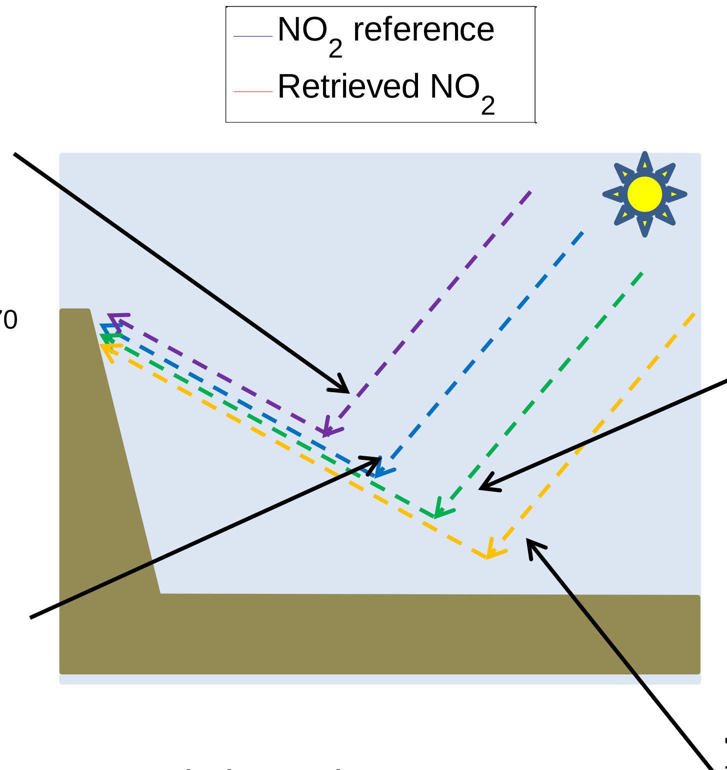

DSCD: (7.3 ±0.1) x 10^{16}

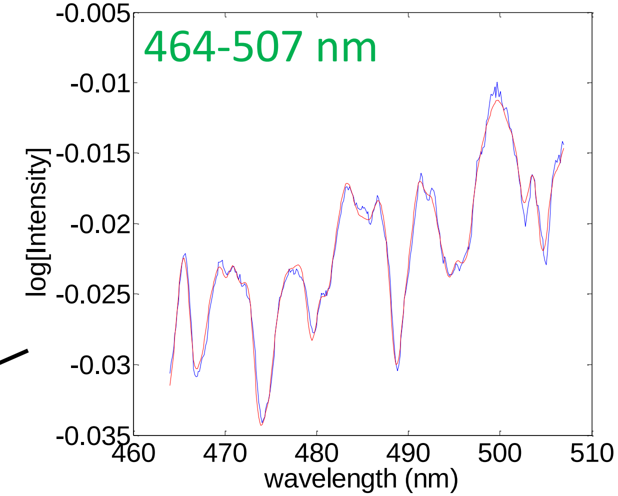

DSCD: (7.4 ± 0.2) x 10^{16}

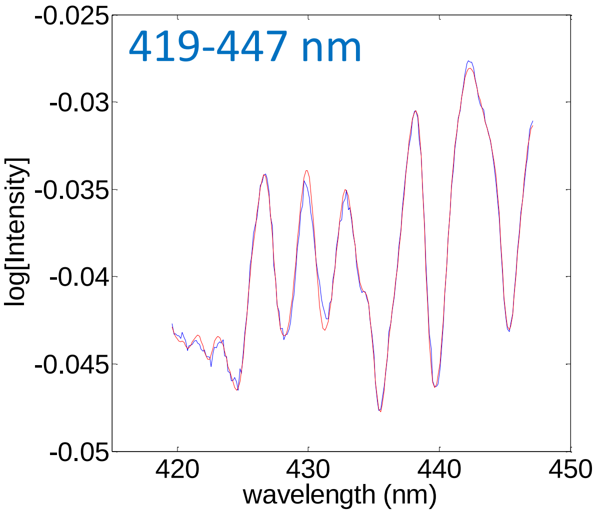

DSCD: (10 ± 0.2) x 10^{16}

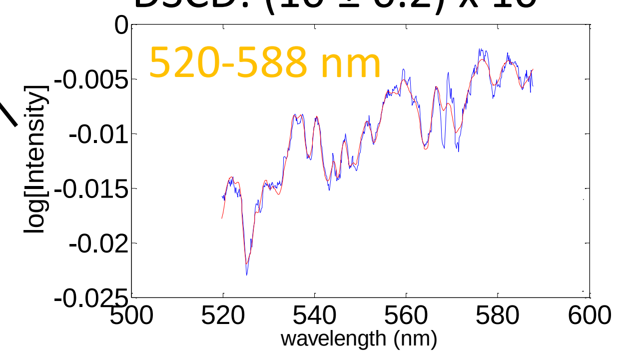

Path length is wavelength dependent due to scattering effects

Comparison to Ground-Based MAX-DOAS

Study	DOFs obtained	Notes
Wang., T., et al., 2014	0.7-2.1	SO_2 retrievals
Sinreich, R, et al., 2013	~1	Parameterized method
Coburn et al., 2013	~2	NO_2, similar method to ours
Vlemmix, T., et al., 2011	2-3*	Theoretical NO_2 study with comparisons
Clemer, K., et al., 2010	1.5-2	Multiple-wavelength retrievals
This study (elevated mountaintop position)	~3-5 (aerosol), ~4-6 (NO_2)	Theoretical retrieval
This study (elevated mountaintop position)	~3-4 for aerosols, 3-5 for NO_2.	Typical atmospheric retrievals

We see 2-3 times as much information from a mountaintop position, than can be see from ground

Retrievals of Vertical Profiles: Optimal Estimation

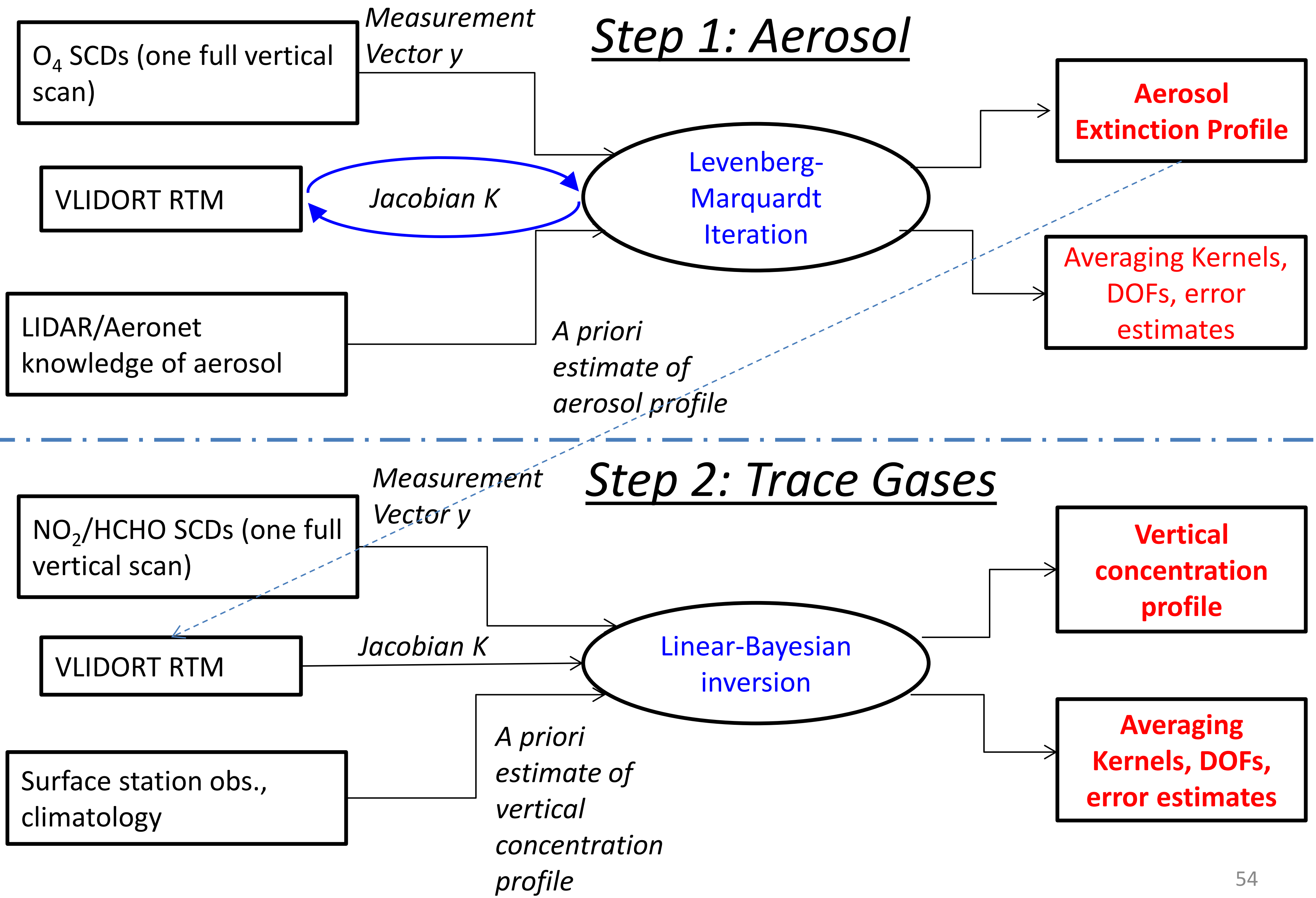

DoF Dependence on Environmental Parameters

		Aerosol Extinction Coefficient (km^{-1})				
		0.05	**0.1**	**0.25**	**0.5**	**1.0**
Boundary Layer Height (km)	**0.1**	**3.66**	**3.63**	**3.56**	**3.41**	**2.93**
	0.5	**3.65**	**3.61**	**3.49**	**3.15**	**2.64**
	1.0	**3.63**	**3.56**	**3.35**	**2.77**	2.09
	1.5	**3.59**	**3.48**	**2.97**	2.82	2.16
	2.0	**3.57**	**3.43**	2.81	2.42	1.62

		Measurement error				
		0.2%	0.5%	1%	2%	5%
A priori error	10%	3.94	3.12	2.37	1.50	0.65
	20%	4.49	3.94	**3.42**	2.65	1.50
	50%	4.89	4.34	3.94	3.42	2.37
	100%	5.23	4.77	4.35	3.94	3.20
	500%	5.73	5.23	4.89	4.49	3.94

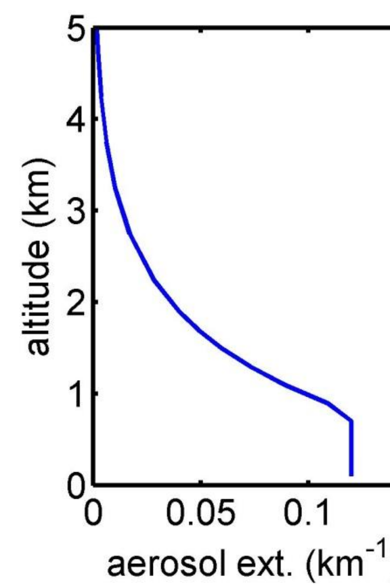

Atmospheric Aerosol Retrievals